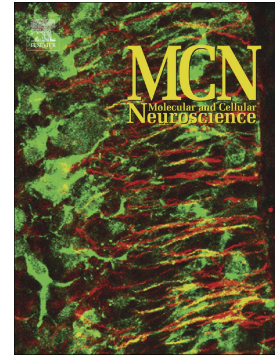


Journal Pre-proof

Modelling Frontotemporal Dementia using patient-derived induced pluripotent stem cells

Georgie Lines, Jackie M. Casey, Elisavet Preza, Selina Wray



PII: S1044-7431(20)30176-7

DOI: <https://doi.org/10.1016/j.mcn.2020.103553>

Reference: YMCNE 103553

To appear in: *Molecular and Cellular Neuroscience*

Received date: 8 February 2020

Revised date: 27 August 2020

Accepted date: 12 September 2020

Please cite this article as: G. Lines, J.M. Casey, E. Preza, et al., Modelling Frontotemporal Dementia using patient-derived induced pluripotent stem cells, *Molecular and Cellular Neuroscience* (2020), <https://doi.org/10.1016/j.mcn.2020.103553>

This is a PDF file of an article that has undergone enhancements after acceptance, such as the addition of a cover page and metadata, and formatting for readability, but it is not yet the definitive version of record. This version will undergo additional copyediting, typesetting and review before it is published in its final form, but we are providing this version to give early visibility of the article. Please note that, during the production process, errors may be discovered which could affect the content, and all legal disclaimers that apply to the journal pertain.

© 2020 Published by Elsevier.

Modelling Frontotemporal Dementia using patient-derived induced pluripotent stem cells

Georgie Lines*, Jackie M. Casey*, Elisavet Preza*, Selina Wray.

Department of Neurodegenerative Disease, UCL Queen Square Institute of Neurology,
University College London, 1 Wakefield Street, London, UK, WC1N 1PJ.

* authors contributed equally

Corresponding author: Selina Wray, PhD
Department of Neurodegenerative Disease
UCL Queen Square Institute of Neurology
London WC1N 1PJ
selina.wray@ucl.ac.uk
020 7672 4297

Abstract

Frontotemporal dementia (FTD) describes a group of clinically heterogeneous conditions that frequently affect people under the age of 65 (1). There are multiple genetic causes of FTD, including coding or splice-site mutations in *MAPT*, *GRN* mutations that lead to haploinsufficiency of progranulin protein, and a hexanucleotide GGGGCC repeat expansion in *C9ORF72*. Pathologically, FTD is characterised by abnormal protein accumulations in neurons and glia. These aggregates can be composed of the microtubule-associated protein tau (observed in FTD with *MAPT* mutations), the DNA/RNA-binding protein TDP-43 (seen in FTD with mutations in *GRN* or *C9ORF72* repeat expansion) or dipeptide proteins generated by repeat associated non-ATG translation of the *C9ORF72* repeat expansion. There are currently no disease-modifying therapies for FTD and the availability of *in vitro* models that recapitulate pathologies in a disease-relevant cell type would accelerate the development of novel therapeutics. It is now possible to generate patient-specific stem cells through the reprogramming of somatic cells from a patient with a genotype/phenotype of interest into induced pluripotent stem cells (iPSCs). iPSCs can subsequently be differentiated into a plethora of cell types including neurons, astrocytes and microglia. Using this approach has allowed researchers to generate *in vitro* models of genetic FTD in human cell types that are largely inaccessible during life. In this review we explore the recent progress in the use of iPSCs to model FTD, and consider the merits, limitations and future prospects of this approach.

Key words: iPSC, FTD, Tau, Progranulin, C9ORF72, TDP-43

Introduction

It is estimated that approximately 50 million people world-wide are currently living with dementia, a figure that is predicted to reach 152 million by 2050 (<https://www.who.int/news-room/fact-sheets/detail/dementia>). Frontotemporal dementia (FTD) accounts for up to 15% of dementia cases, and is the second most common cause of dementia in patients below 65 years of age (2). Around 40% of FTD cases are familial (3), with heritability varying between clinical symptoms (4). FTD is a clinically, genetically and pathologically heterogeneous disorder. The main clinical subtypes of FTD are behavioral variant FTD (bvFTD) and primary progressive aphasia (PPA), which are characterized by changes in behavior and language deficits respectively (5). FTD also clinically overlaps with a number of motor disorders including progressive supranuclear palsy (PSP), corticobasal syndrome (CBS), parkinsonian disorders (FTD-PD), and motor-neuron disease (FTD-MND or FTD-ALS) (4). Multiple genetic causes of familial FTD have been identified. The most common mutations associated with FTD are in the genes encoding the microtubule-associated protein tau; *MAPT* (6-9), progranulin; *GRN* (10, 11), and *C9ORF72* (12, 13). Rarer causative mutations in *VCP* (14, 15), *TARDBP* (16) and *CHMP2B* (17) have also been identified. The pathology of FTD can be classified according to the constitution of its protein inclusions. FTLD-tau accounts for 30-50% of FTD cases (18-20) and is pathologically identified by the presence of tau-positive inclusions which are a hallmark of FTD with *MAPT* mutations (21, 22). FTLD-TDP occurs in 50-60% of FTD patients (18-20) and displays tau-negative but ubiquitin /TDP-43 positive inclusions. FTLD-TDP pathology is present in cases of FTD with *GRN* mutations (23), *VCP* mutations (24, 25), *TARDBP* mutations (26) and *C9ORF72* repeat expansions (24, 27). The third major histological category, FTLD-FUS, occurs in around 10% of FTD cases

(28). Protein inclusions in FTLD-FUS are tau negative, TDP-43 negative, ubiquitin-positive, FUS (fused in sarcoma) positive (29).

Overlap in the genetics, clinical symptoms and pathology between FTD and ALS have led to the interpretation that ALS and FTD are two diseases on a single spectrum (30). Indeed, patients with FTD can develop motor deficits (1, 5). Lashley et al. have written a thorough overview of the clinical, genetic and pathological heterogeneity in FTD (31). There are currently no disease-modifying treatments for FTD. This may be due, in part, to a lack of disease models that accurately recapitulate the complex pathologies of the disease. Progress towards a disease-modifying therapy would be greatly enhanced by the availability of disease models which reliably recapitulate disease pathologies in the cell type(s) that degenerate in disease.

The ability to reprogram somatic cells into induced pluripotent stem cells (iPSCs) has revolutionised *in vitro* disease modelling, particularly for neurological disorders where *in vitro* cultures of human neurons are not available. Briefly, somatic cells such as fibroblasts or peripheral blood mononuclear cells can be taken from a person with a genotype/phenotype of interest, and reprogrammed to a pluripotent state by the exogenous expression of the pluripotency-associated transcription factors Oct4, Klf4, Sox2 and cMyc (32). The resulting iPSCs can be subsequently differentiated into disease-relevant cell types, including multiple subclasses of neurons, astrocytes and microglia, thus permitting the generation of disease models which contain the patient's precise genome in the cell type that selectively degenerates (Figure 1). These human iPSC-neurons have the advantage of endogenous expression of the mutant gene of interest, in the cell type specifically affected by disease.

Here, we will review insights into genetic FTD that have been gained through the use of iPSCs and discuss future directions and challenges.

iPSC models of *MAPT* mutations

Tau pathology and the *MAPT* gene

Hyperphosphorylated, insoluble aggregates of the microtubule associated protein tau are the pathological hallmark of a range of clinically diverse neurodegenerative diseases collectively termed the tauopathies (21). Alzheimer's Disease (AD) is the most common of these diseases, although AD is widely accepted to be a secondary tauopathy, as genetic and *in vivo* evidence supports the notion that tau pathology is downstream of amyloid (33-35). Even so, multiple lines of evidence suggest tau dysfunction is essential to neurodegeneration in AD. Tau pathology spreads in a well-defined manner and correlates with clinical severity and the extent of neurodegeneration (36-39). Further, tau knockout rodents are largely protected against amyloid toxicity (40-43). The primary tauopathies, where tau is the defining pathological feature, include progressive supranuclear palsy (PSP), corticobasal degeneration (CBD) and FTD linked to mutations in *MAPT* (21). However, it was the discovery of causative mutations in *MAPT* linked to FTD that provided confirmation that tau dysfunction was sufficient to cause neurodegeneration (6-9).

The tau protein is encoded for by the *MAPT* gene, located on chromosome 17q21.31. *MAPT* consists of 16 exons, and alternative splicing of exons 2, 3, and 10 results in the generation of multiple tau isoforms in the adult CNS. These differ in the inclusion of 0, 1 or 2 N terminal repeats (0N, 1N and 2N), encoded by exons 2 and 3, and in the presence of 3 or 4 C-terminal microtubule binding domains (3R or 4R) encoded by exon 10. Exon 3 is not translated without exon 2, therefore six protein isoforms are generated: 0N3R, 0N4R, 1N3R, 1N4R,

2N3R and 2N4R (44-47). The levels of 3R and 4R tau are approximately equal in the healthy adult human CNS (46, 48).

Over 40 mutations in *MAPT* linked to FTD have been described, and these can either affect the coding sequence or result in altered tau splicing. The majority of mutations are clustered between exons 9-13, within and around the microtubule binding repeats. *MAPT* missense mutations associated with FTD have been identified in exons 1, and 9 to 13. Such mutations (e.g. G272V, P301L, P301S, V337M, R406W) do not influence tau splicing, however they have been shown to decrease the ability of tau to bind to microtubules (49) and increase tau aggregation, resulting in neurodegeneration (50). Mutations located in intron 10 of the *MAPT* gene (10+3, 10+11, 10+12, 10+13, 10+14, and 10+17) cause a dysregulation of *MAPT* splicing. These mutations destabilise a stem loop structure, unmasking the 5' splice site, resulting in the increased inclusion of exon 10, and an increase in the 4R:3R tau ratio (51). Additionally, there are a number of mutations present in exon 10 that also disrupt the 4R:3R tau ratio by altering splicing enhancers (N279K) or suppressors (L284L and N296H) (52-56). Mutations that cause an imbalance of the 3R/4R tau ratio are sufficient to cause tauopathies (7, 9, 51, 57), but the mechanisms of how these mutations cause neurodegeneration has not yet been elucidated. The composition of tau pathology in FTD varies depending on the mutation and isoforms affected, and can either consist of all 6 tau isoforms in paired helical filaments, or a subset of isoforms such as 4R-only pathology (31).

The generation of appropriate models to investigate the molecular mechanisms underpinning tauopathies such as FTD has been challenging, as immortalised cell lines and animal models do not recapitulate the complex pattern of *MAPT* splicing seen in the adult human CNS. For example, in the adult murine brain, tau only exists in three isoforms, each with 4R

microtubule binding domains (0N4R, 1N4R and 2N4R) (58). Additionally, many studies have relied on tau overexpression models to investigate the proteins role in disease, however this can lead to extreme phenotypes, such as the clogging of axons and re-organisation of the neuronal cytoskeleton, which are not truly reflective of endogenous tau expression in disease (59). Primary human neurons have been shown to correctly express all tau isoforms, however these are not widely used due to the limited availability of aborted fetal tissue (60). Thus, iPSC-neurons provide an attractive model system to study the effect of tau mutations at the endogenous level, and a wide range of iPSCs from tauopathy patients are now accessible to the field (61).

Tau splicing in iPSC-neurons

Tau splicing is developmentally regulated and proper stoichiometry of tau isoforms appears to be critical for neuronal health (7, 62). In the fetal stages of development, only the shortest tau isoform, 0N3R, is expressed, however in the post-natal CNS, all six isoforms are present (45, 47).

Multiple studies using comparative transcriptomics have demonstrated that iPSC-neurons closely resemble fetal neurons, at least in terms of global gene expression profiles (63, 64). This raises the question of whether iPSC-neurons express the full complement of tau isoforms present in the adult human brain, and several groups have investigated this. Sposito et al. demonstrated that control iPSC-cortical neurons express mainly the fetal tau isoform (0N3R from D20 to D100) (65). However, neurons cultured for 365 days showed a switch in tau splicing from exclusively 0N3R, to 0N3R, 0N4R, 1N3R and 1N4R. Interestingly, Sposito et al. did not observe the presence of 2N tau, which is the least abundant isoform in the CNS, accounting for only 9 % of total tau, although this could be due to sensitivity of the detection

method. Other studies have reported the expression of exon-10 containing tau isoforms from 4-10 weeks in iPSC-dopaminergic and mixed neuronal populations (66-69). These differences in *MAPT* splicing between studies may be driven by the use of different differentiation protocols, neuronal subtype specific regulation of *MAPT* splicing, or differences in the sensitivity of methods used to detect tau. However, these studies have important implications for modelling tauopathies, as they demonstrate that iPSC-neurons have the ability to recapitulate the complex developmental splicing of *MAPT*, and express multiple tau isoforms.

The use of mass spectrometry can provide sensitive and unambiguous identification of tau isoforms. Paonessa et al. reported expression of 3R and 4R tau after 120 days using non-quantitative mass spectrometry (70). Sato et al. developed a stable isotope labelling kinetics (SILK) quantitative mass spectrometry protocol to examine tau production and turnover (71). They demonstrated that iPSC-neurons express lower levels of 4R tau and have a faster tau turnover rate (6 days) when compared to the human brain (23 days). 4R tau and phosphorylated tau was degraded faster than 3R and non-phosphorylated tau in iPSC-neurons, suggesting unique processing of these tau species.

The full impact of differentiation protocol and cell culture conditions remains to be determined. Interestingly, in a chimeric model, whereby human iPSC-neurons are transplanted into mouse frontal cortex, iPSC-neurons express equimolar levels of 3R and 4R tau at 6 months post injection (72). This work suggests that iPSC-neurons may mature faster in an *in vivo* environment, with a combination of cell types and increased structural diversity. Several groups have reported a more mature tau expression profile in 3D cultures, including a

3D neuronal culture derived from immortalised neuronal progenitor cells (73), and a 3D iPSC-neuronal system (74).

Several protocols have been established for the culture of 3D organoids from iPSCs (75), resulting in self-organising neuronal structures that can recapitulate fetal brain development (76-79). It is also possible to directly convert fibroblasts into neurons by the exogenous expression of pro-neuronal transcription factors in a process known as transdifferentiation (80). This has been shown to promote the retention of biological signals of aging, suggesting that transdifferentiated neurons may be more mature than those converted from iPSCs (81). Tau splicing in organoids and neurons generated by transdifferentiation has not yet been investigated.

Despite the apparent fetal nature of iPSC-neurons, they have been successfully used by multiple groups to investigate mutations that affect tau splicing (summarised in Table 1). Multiple studies have shown that iPSC-neurons with intron 10 splicing mutations, 10+16 and 10+14, express 4R tau isoforms significantly earlier than controls (65, 82, 83). Similar results have been determined in neurons carrying the exon 10 N279K missense mutation, which also increases the 4R:3R tau ratio at early developmental timepoints (67, 84, 85). These results indicate that mutations that alter *MAPT* splicing can override the developmental regulation of tau isoforms.

Investigating mechanisms of tau-mediated neurodegeneration in iPSC-neurons

i) Tau pathology

Multiple reports have examined neurons with *MAPT* mutations for hallmarks of tau pathology, including hyperphosphorylation, detergent insolubility and formation of aggregates (Figure 2). Tau phosphorylation has been reported to be significantly higher than controls in iPSC-neurons carrying *MAPT* mutations including 10+16, P301L, N279K, and

V337M (67, 70, 84). In all these cases phosphorylation was increased at S202 and T205 (as detected by AT8 antibody), epitopes that are typically hyperphosphorylated in tauopathies (86, 87), but not in the developing brain (88). Interestingly Nakamura et al. report that in R406W iPSC-neurons, tau isotopes S404 and S409 are less phosphorylated compared to control neurons (89). Further investigation revealed that the R406W mutation impaired the phosphorylation of S404 by GSK and CDK5, and S409 by Rho-associated protein kinase and protein kinase A (89). Tau phosphorylation is also developmentally regulated, and multiple epitopes in human (88) and mouse brain (90) show higher phosphorylation at early developmental stages. Thus, it is also important to consider the fetal identity of iPSC-neurons and how this may impact on assigning disease-associated phosphorylation events.

Imamura et al. reported that 10+14 and R406W iPSC-neurons displayed an accumulation of intracellular misfolded tau detected using the anti-oligomeric tau antibody, TOC1 (82). Interestingly, the high molecular weight species observed in 10+14 cell lysates, were not the same as those observed in R406W cell lysates. This suggests that the conformation of misfolded tau is not uniform between mutations, which could contribute to the heterogeneity seen in FTD. Iovino et al. demonstrated that iPSC-neurons with N279K mutations displayed occasional dot-like structures when stained with a phosphorylated S212 and S214 antibody (AT100), indicating filamentous tau aggregates. These aggregates were only observed in N279K neurons, not in controls or in P301L mutation neurons (67).

These data collectively demonstrate the ability of iPSC-neurons to model early stages of tau pathology. However, so far the presence of tau tangles in *MAPT* mutation neurons (by Gallyas positive staining or visualisation of tau filaments) has not been demonstrated, even in cell lines where multiple *MAPT* mutations have been engineered (91).

ii) Tau seeding and spread

Braak and Braak postulated that tau pathology spreads from one brain region to another, contributing to progressive white matter loss, as evidenced by pathology studies which show tau pathology progresses in a predictable sequence that correlates with neurodegeneration and the extent of dementia (36). This has promoted numerous studies investigating the transcellular spreading of tau in disease, which are reviewed in Demaegd et al. (92). Recently, iPSCs have begun to be utilized to model tau spread. Tau can be released from wild-type iPSC-neurons into the extracellular space and taken up trans-neuronally by primary neurons (93). Evans et al. reported that monomeric wild type and P301S tau, and aggregated P301S tau, can efficiently enter iPSC-neurons by endocytosis, suggesting that tau spread is a biological event, not a necessarily a disease-specific phenomenon (94). Interestingly, Sato and colleagues demonstrated that in human iPSC-neurons, newly synthesized tau is truncated and released into the media after 3 days, further suggesting that tau release is a regulated, physiological event (71).

iii) Alterations in neuronal morphology

A range of morphological differences have been observed in iPSC-neurons carrying *MAPT* mutations (Figure 2). P301L neurons exhibited thicker, contorted processes with varicosity structures containing alpha synuclein and 4R tau deposits (67), a feature that could also be observed in post-mortem tissue from the same patient. An increased frequency of nuclear lamina invaginations and folds was observed in 10+16 and P301L iPSC-neurons and post mortem tissue from 10+16 mutation donors (70). iPSC-neurons with N279K and V337M mutations displayed significantly shorter neurites compared to controls (84). In addition, N279K and V337M neurons showed a significant increase in tau fragmentation at the

expense of full-length tau, which may be contributing to the disturbed neurite morphology (84).

iv) Transport and function of mitochondria

Tau mis-localisation from the axons, to the cell body and dendrites was reported in iPSC-neurons carrying 10+16 and R406W mutations (70, 89). The primary function of tau is to stabilize microtubules, which are essential for the anterograde and retrograde transport of cargo along the axon (95). Hyperphosphorylation and redistribution of tau may impede its ability to stabilise microtubules, resulting in an impairment in axonal transport, and eventually axonal degeneration.

The transport of mitochondria throughout neurons is essential for the maintenance of normal cellular function, as neurons have high energy demands, requiring large amounts of ATP (96). As such, disruption of mitochondrial transport, and mitochondria activity in general, have been implicated in the pathogenesis of numerous neurodegenerative diseases (97).

Iovino et al. reported more stationary mitochondria in N279K and P301L neurons, in addition to a reduction in anterogradely moving mitochondria in N279K and P301L neurons by 23% and 15.3 % respectively (67). In contrast to this finding, Nakamura et al. observed an increase in mitochondria movement in R406W neurons, with more mitochondria moving in the retrograde direction compared to controls. It has previously been reported that the microtubule binding domain of tau has the ability to inhibit the motility of kinesin and dynein (98). Nakamura et al. therefore suggested that the dissociation of mutant tau from microtubules promotes dynein to become more motile, resulting in increased retrograde transport (89). Alternatively, differences may be due to unknown molecular effects driven by different tau mutations.

Elevated reactive oxygen species (ROS) can directly damage macromolecules, membranes and organelles which have deleterious consequences on the effected cell. Increased mitochondrial membrane potential was observed in 10+16 iPSC-neurons, leading to the overproduction of ROS in mitochondria, oxidative stress and cell death (99). Cell death was prevented by the addition of mitochondrial antioxidants, suggesting that damage caused by mitochondrial ROS is a key facilitator of neurodegeneration. Ehrlich et al. also demonstrated that N279K neurons display a significant increase in the release of lactate dehydrogenase after rotenone treatment, suggesting an increased sensitivity to oxidative stress. This was also confirmed by a reduction in cell death after neurons were treated with antioxidants (84).

Biswas et al. reported an increase in MMP-9 and MMP-2, Zn containing proteolytic enzymes, in iPSC-neurons with 10+16 and G152T mutations (100). These neurons displayed an increased sensitivity to the cell stressor rapamycin, and treatment of control neurons with MMP-9 and MMP-2 was enough to induce cell death, suggesting MMP-9 and MMP-2 may play a role in neurodegeneration. Interestingly, these results are consistent with a publication (101) which reports that MMP-9 contributes to neuronal vulnerability in ALS, strengthening the idea that FTD and ALS are two diseases on a single spectrum.

v) Neuronal function

Neurons carrying the N279K and P301L mutations revealed an earlier neuronal maturation compared to controls (67), suggesting a link between tau dysfunction and neuronal activity. Further evidence for this is provided by Imamura et al., who demonstrated that 10+14 neurons evoked an elevated calcium transient compared to controls when stimulated, indicating increased electrical activity of mutant neurons (82). Additionally, transcriptomic

analysis of neurons with the R406W mutation revealed reduced expression of GABA receptors (102). In characterising 10+16 and A152T (a risk modifying mutation) iPSC-neurons, Biswas et al. reported that when treated with tetrodotoxin, both mutant cultures exhibited an increased number of neurons that responded with action potentials (100). Tau release from neurons is positively modulated by neuronal activity (103), therefore it is tempting to speculate that earlier, more frequent, and stronger electrical activity of mutant neurons could be contributing to the development and spread of tau pathology.

vi) Modelling tau variants that increase risk of tauopathy

The mutations discussed above (10+16, 10+14, N279K, V337M, R406W) are all causative of FTD. The A152T variant has recently been shown to increase risk of tauopathy (104, 105). iPSC-neurons with the A152T variant display prominent neurodegenerative phenotypes, such as increased tau fragmentation and phosphorylation, tau mislocalization and axonal degeneration (106-108). It is curious that such strong phenotypes can be observed in relatively young neurons with a variant that is a risk-modifier rather than a causative mutation, however similar phenotypes have also been reported in patients with the A152T mutation (106). It is also possible that cellular phenotypes are exacerbated *in vitro* due to a lack of other cell types, such as astrocytes, which would normally provide trophic support. Importantly, Silva et al. demonstrated that tau accumulation and phosphorylation phenotypes these phenotypes could be rescued in A152T neurons following the targeted degradation of tau (108). In addition Silva et al. showed that degradation of tau prevented cell death of A152T neurons after A β (1-42) treatment (108).

The *MAPT* gene sits in the largest known region of linkage disequilibrium in the human genome, where two major haplotypes exist: H1 and H2 (109). The H1 haplotype confers

increased risk for PSP and CBD (110). Both PSP and CBD are characterised by selective deposition of 4R tau isoforms, and therefore it is possible that H1/H2 have haplotype-specific effects on tau expression and splicing (111, 112). Beevers et al. demonstrated that mature dopaminergic iPSC-neurons show haplotype differences in *MAPT* expression, with H1 haplotypes expressing 22% higher levels of *MAPT* than H2 (69). No changes in exon 10 expression associated with *MAPT* haplotype were observed.

iPSC models of FTD associated with TDP-43 pathology

TDP-43 pathology and the *TARDBP* gene

Mutations in *TARDBP*, the gene that encodes Transactive response DNA-binding protein 43 (TDP-43), can cause both ALS and FTD (26, 113). TDP-43 is a ubiquitously expressed RNA/DNA binding protein, which is the main constituent of the ubiquitinated inclusions found in the cytoplasm and nucleus in the majority of ALS patients and approximately 50% of FTD patients (FTLD-TDP) (114-117). TDP-43 pathology is found in familial FTD caused by mutations in *GRN*, *C9ORF72*, and *VCP* (23-25, 27). Although, *TARDBP* mutations are more commonly associated with ALS, they can also cause FTD (16, 26, 118, 119) and due to the clinical and pathological overlap these models are also relevant to understanding FTD and have therefore been included in this review. TDP-43 inclusions and/or alterations have also been linked to a number of other diseases and injuries, including Alzheimer's Disease, Niemann-Pick C and Traumatic Brain Injury (120-125). TDP-43 can undergo a number of post-translational modifications (PTMs) that affect its function, with the PTM profile and resulting pathology appearing to be disease-specific. Although detection methods limit our identification and knowledge of the effect of certain PTMs, some of the most common disease-associated modifications identified in the ALS/FTD spectrum are; phosphorylation, acetylation, cysteine oxidation, ubiquitination and the generation of C-terminal domains

(125). Phosphorylation of TDP-43 reduces its solubility (126). Cohen et al. found that acetylation resulted in hyper-phosphorylated, aggregated TDP-43, with reduced RNA binding (127). Ubiquitination of TDP-43 has also been found to affect its interaction with p62, which may play a role in clearing TDP-43, with lower rates of coimmunoprecipitation in FTLD-TDP patients than controls (128). C-terminal TDP-43 fragments (25kDa and 35kDa) commonly identified in ALS and FTD lack the nuclear localization signal, which is likely to affect localization and movement between the nucleus and cytoplasm (125, 129).

iPSC models of FTD caused by mutations in *GRN*

***GRN* mutations in FTD**

GRN is located on chromosome 17q21, in the same region as *MAPT*, and codes for the progranulin protein (10, 11). Mutations in the *GRN* gene that cause haploinsufficiency of progranulin account for 5-10% of all frontotemporal dementia cases (1) and lead to FTD with TDP-43 pathology (23, 130, 131). *GRN* mutations that result in FTD, such as nonsense mutations, splice-site mutations and deletions, have been identified throughout the gene (www.molgen.vib-ua.be/FTDmutations). However, there is significant variability in the age of onset and disease progression, even for patients with the same mutation (130-134).

Progranulin is an 88 kDa secreted glycoprotein, expressed in the brain by both neurons and glia. When progranulin is internalised by cells it can be cleaved to generate seven and a half smaller peptides termed granulins, thought to be the intracellular functional units of progranulin (135-138). Multiple functions for progranulin/granulins have been suggested, including the regulation of neuronal differentiation and neurite outgrowth, synaptogenesis, inflammation and wound repair (136, 139-141). More recently, a role for progranulin in lysosome function has emerged. Complete loss of progranulin causes a lysosomal storage disorder, Neuronal Ceroid Lipofuscinosis (NCL) (142-144). Lysosomal dysfunction is also

observed in patients with heterozygous progranulin mutations (145, 146), as well as progranulin knock-out mice (147, 148). Cleavage of progranulin into the individual granulins is mediated in the lysosome by cathepsins B and L, and progranulin/granulins can regulate the activity of several lysosomal enzymes including glucocerebrosidase (GBA) and cathepsin D (138, 149-153). Cathepsin D activity is upregulated in *GRN*^{-/-} mice and pull down assays have identified an interaction between progranulin and cathepsin D (150). TDP-43 aggregates have also been detected in mice deficient in cathepsin D and both mice and humans with cathepsin D (CTSD) mutations exhibit symptoms of NCL (145, 154, 155)

iPSC-neurons with *GRN* mutations

*i) Progranulin haploinsufficiency and mislocalised TDP-43 in *GRN* iPSC-neurons*

Almeida et al. generated iPSC-neurons from a patient with a heterozygous *GRN* nonsense mutation (S116X), a healthy control and a sporadic FTD patient (156). *GRN* mRNA was reduced by 41% and intracellular and extracellular progranulin protein levels were reduced by approximately 50% in the *GRN* mutation iPSC-neurons, compared to the healthy and sporadic FTD controls. This demonstrates that patient-derived neurons are a good model of progranulin haploinsufficiency. Mutant *GRN* iPSC-neurons exhibited an increased sensitivity to tunicamycin and lactacystin, which inhibit protein N-glycosylation and proteasome activity respectively. *GRN* S116X iPSC-neurons also showed increased sensitivity to staurosporine, a broad spectrum kinase inhibitor. Cytoplasmic TDP-43 was increased in the *GRN* S116X iPSC-neurons, in line with previous findings that increased caspase-3 leads to higher levels of cleavage and mislocalisation of TDP-43 (157), demonstrating that iPSC-neurons from *GRN* patients can recapitulate the main disease pathology of *GRN* mutation FTD. These phenotypes were proposed to be due to progranulin haploinsufficiency affecting the PI3K/AKT and MEK/MAPK signaling axis.

ii) Modulating progranulin levels in GRN iPSC-neurons

As all *GRN* mutations result in progranulin haploinsufficiency, methods to restore progranulin levels provide an attractive therapeutic strategy. Several groups have used iPSC-neurons to investigate strategies to upregulate progranulin levels. In Almeida et al.'s (2012) study the increased sensitivity to inhibitors of the PI3K/AKT and MEK/MAPK pathways was rescued by exogenous introduction of *GRN* to restore progranulin levels. A number of follow-up studies used the same iPSC lines as this initial study (153-161). Lee et al. tested methods of preventing binding of progranulin to sortilin (158). Sortilin is a neuronal receptor that can internalise progranulin by endocytosis and regulate its trafficking to the lysosome (162). They identified amino acids 588-593 of progranulin as the region where sortilin binds and developed small molecules to prevent this interaction, resulting in an increase in extracellular progranulin levels by blocking progranulin uptake. Although this increased extracellular progranulin levels, the impact of reduced lysosomal progranulin/granulins was not explored. Almeida et al. found that 24-hour treatment of 2 week old iPSC-derived cortical neurons with suberoylanilide hydroxamic acid (SAHA) increased levels of *GRN* mRNA and protein in all control, sporadic FTD, and S116X mutation lines without affecting survival rates (160). Unfortunately, as SAHA is a histone deacetylase inhibitor and affects the expression of many genes, it is unlikely to be suitable as a therapeutic. Another study by Holler et al. found that progranulin was increased in iPSC-neurons treated with trehalose, a disaccharide that activates autophagy independently of the mTOR signalling pathway (163). Genetic screens in primary neurons and neuroblastoma lines have identified further modifiers of progranulin levels, including *RIPK1* and *TRAP1* (164, 165). The development of CRISPR-based interference screens will enable further identification of genetic modifiers of progranulin levels in human neurons (166).

iii) Altered neuronal development and neuronal function in GRN iPSC-neurons

Gascon et al. examined the levels of miR-124 and AMPA receptors (AMPARs) in iPSC lines from a *GRN* (S116X) patient and two *C9ORF72* repeat expansion patients with bvFTD (159). MiR-124 is a small non-coding RNA that plays a role in neural development, and is predicted to target GluA2, GluA3 and GluA4 (167, 168). Gascon et al. found no difference in miR-124 levels at 2 weeks post differentiation but reduced miR-124 levels and increased GluA2 and GluA4 AMPAR subunits in 8 week old S116X neurons, compared to controls. This would likely result in an increase in Ca²⁺ impermeable AMPARs as GluA2 subunits are Ca²⁺ impermeable. They also found a decrease in miR-124 levels and associated increases in GluA2 and GluA4 AMPAR subunits in the frontal cortices of patients with sporadic bvFTD and *GRN* haploinsufficiency mutations. They did not detect any difference in NMDA receptors, kainate receptors or miR-9 levels between the groups. Other studies have also found that miR-124 suppresses the expression of GluA2 receptor subunits (169, 170).

Raitano et al. generated iPSCs and then cortical neurons from three patients with a *GRN* (IVS1+5G>C) mutation (171). When compared with embryonic stem cells and control iPSCs, they observed less efficient cortical neuronal differentiation in the *GRN* lines, with only a small proportion expressing *TUBB3* mRNA, but no difference in neural progenitor or motor neuron differentiation efficiency. This impairment in cortical neuronal differentiation efficiency was rescued by restoration of progranulin levels. This finding is in contrast to the initial Almeida et al. study, which found similar rates of differentiation and no difference in the proportion of cells positive for neuronal or astrocytic markers (156). However, Almeida et al. used a protocol to produce a mixed neuronal population and characterised them between 2-4 weeks, whereas Raitano et al. did not identify differences until D40 *in vitro* and used a

protocol to produce predominantly cortical neurons. This could suggest progranulin has a specific role in cortical neuron differentiation.

iv) Lysosomal dysfunction in GRN iPSC-neurons

The lysosomal function of progranulin has gained recent attention and warrants investigation in iPSC models. Lee et al. found that progranulin was localised to the lysosome where it co-localised with cathepsin L, a lysosomal cysteine protease (161). Complementary approaches using cathepsin overexpression and pharmacological inhibition support a role of cathepsin L in the cleavage of progranulin into granulins in the lysosome. In addition to being a substrate for cathepsins, progranulin/granulins may also regulate cathepsin maturation and activity. Valdez et al. found decreased cathepsin D activity but no difference in the levels of mature cathepsin D, cathepsin B activity or cathepsin L activity in iPSC-cortical neurons with the A9D *GRN* mutation (151). They identified granulin E, specifically, as an activator of cathepsin D. They also found decreased nuclear TDP-43, along with an increase in insoluble TDP-43. CRISPR/Cas9 correction of the mutation to generate an isogenic control ameliorated these phenotypes. These studies suggest that cathepsin L regulates the levels of full-length progranulin and individual granulins, whereas progranulin regulates cathepsin D activity.

iPSC-derived neurons generated from patients with *GRN* mutations display many of the pathological phenotypes seen in patients (summarised in Table 2 and Figure 3). To date, these studies have been largely restricted to iPSC-neurons. However, accumulating evidence suggests loss of progranulin disrupts microglia function. Transcriptomics of *GRN* knockout mice revealed specific alterations in microglia that were absent from neurons (172) and a further study showed the microglial signature from *GRN* $-/-$ mice is similar to those isolated

from neurodegenerative disease brain (173). Loss of progranulin appears to be associated with altered lipid metabolism, leading to an accumulation of polyunsaturated triacylglycerides in knockout mice (174) and a genetic screen identified *GRN* as a genetic modifier of lipid droplet formation in microglia (175). Future studies investigating the cell-type specific consequences of progranulin haploinsufficiency in iPSC-microglia are eagerly anticipated, and robust protocols have recently been optimised to enable this (176). Further, the contribution of progranulin versus individual granulins to disease aetiology has not been fully dissected and remains an important knowledge gap for investigation in patient cells.

iPSC models of FTD caused by a repeat expansion in *C9ORF72*

The GGGGCC hexanucleotide repeat expansion (HRE) in the first intron of *C9ORF72* is the most common genetic cause of both FTD and amyotrophic lateral sclerosis (ALS) (12, 13). The overall mutation frequency of *C9ORF72* is 20% for familial FTD, 16% for familial ALS and around 6%–8% for sporadic ALS and FTD (177). Unaffected individuals usually carry 2–23 repeats in *C9ORF72*, whereas an arbitrary cut off of 30 repeats is commonly used as the pathogenic repeat size threshold (178, 179). *C9ORF72* has three main pre-mRNA transcripts (V1, V2 and V3) producing the two main *C9ORF72* protein isoforms, a 481 amino acid long isoform (C9-L) and a 227 amino acid short isoform (C9-S). *C9ORF72* has high homology to Differentially Expressed in Normal and Neoplasia (DENN) related proteins, which act as GDP/GTP exchange factors (GEFs) that activate Rab-GTPases (180). Several lines of evidence suggest that *C9ORF72* is involved in autophagy and lysosomal trafficking (181–189) but little is known about the distinct functions of the two *C9ORF72* protein isoforms. The *C9ORF72* HRE is located in the first intron of *C9ORF72* and following transcription and alternative splicing, V1 and V3 transcripts contain the intronic repeat, but not V2, resulting in different potential pathogenic mechanisms. Studies on *C9ORF72* HRE patient tissue have shown that the HRE leads to (i) a reduction in *C9ORF72* mRNA V2 transcript (13, 190, 191),

(ii) the formation of sense and antisense RNA foci, produced via bi-directional transcription of the *C9ORF72* HRE from transcripts V1 and V3, which may subsequently sequester RNA-binding proteins (12, 13, 192), and (iii) the production of aggregation-prone dipeptide repeat proteins (DPRs) via repeat-associated, non-ATG (RAN) translation of both sense and anti-sense expanded RNA transcripts in all reading frames (Gly-Ala, Gly-Pro, Pro-Ala, Gly-Arg and Pro-Arg) (193-195). These findings altogether have led to the hypothesis that *C9ORF72* HRE causes FTD/ALS by three potential mechanisms; loss of *C9ORF72* function, toxic gain of RNA function or toxic gain of DPR function respectively.

Using iPSCs to model the underlying molecular aetiology of the *C9ORF72* repeat expansion is an attractive approach, as it offers the advantage of fully recapitulating the pathological repeat expansion size present in *C9ORF72* HFE carriers. Nonetheless, it is also challenging as similar to other repeat expansions, the *C9ORF72* HRE is prone to genomic instability (196) leading to HRE mosaicism which is an additional source of genetic heterogeneity in iPSC cultures. Examples of HRE genomic instability and subsequent mosaicism in cell cultures are evident across published *C9ORF72* iPSC studies (197-201). Moreover, all three potential disease mechanisms leading to neurodegenerative phenotypes co-exist in patient-derived iPSC models, and although this adds to their physiological relevance, the contribution of each to cellular phenotypes cannot be easily dissected. Here, we provide a comprehensive review of *C9ORF72* iPSC studies and their findings, which are also summarised in Table 3 and illustrated in Figure 4.

i) Capturing the pathology of C9ORF72 FTD in iPSC-neurons

Since the discovery of *C9ORF72* gene as the major genetic cause of FTD/ALS almost a decade ago, several iPSC studies have emerged that recapitulate some of the major

pathological hallmarks of C9-FTD/ALS. Multiple groups have shown the presence of sense and/or antisense RNA foci in the nuclei of *C9ORF72* patient-derived cortical neurons (197, 202, 203), mixed neurons (204), motor neurons (MNs) (198, 199, 202, 205-207) and astrocytes (208). Importantly, some of these iPSC studies have demonstrated that RNA foci can sequester RNA binding proteins such as RNA-editing deaminase-2 (ADARB2) (204), heterogeneous nuclear ribonucleoprotein A1 (hnRNPA1) and purine-rich binding protein- α (Pur- α) (198) as well as other proteins such as Ran GTPase activating Protein 1 (RANGAP1) (209). It is not known whether this expanded RNA-mediated toxicity is the major driver of neurodegeneration in C9-FTD/ALS similar to what is known for the sequestration of muscleblind proteins by the CUG repeats in myotonic dystrophy (210).

In addition to the presence of RNA foci, DPRs have been identified in iPSC-neurons by multiple studies (197, 199, 202-205, 207, 208). Evidence for cell-to-cell transmission of DPRs was provided by Westergard et al. who showed transmission of poly-GA and poly-GR to control spinal MNs using co-culture and conditioned media from *C9ORF72* patient-derived spinal MNs (211).

Finally, *C9ORF72* haploinsufficiency has also been observed in *C9ORF72* HRE neurons via a reduction in *C9ORF72* transcript expression (197, 204) or in *C9ORF72* protein levels (189, 212, 213). Loss of *C9ORF72* can be caused epigenetically due to the presence of the CpG-rich HRE via extensive DNA methylation of CpG residues at the promoter region of the gene. Indeed, hypermethylation of the *C9ORF72* promoter region, consisting of the *C9ORF72* HRE and its flanking CpG islands, is a frequent finding in patient brain and blood (214-217) and has been reported as a disease modifier in ALS/FTD (218). To date, only a limited number of studies have assessed DNA methylation in *C9ORF72* HRE iPSC models

(200, 207, 219). The first iPSC study to assess DNA methylation and hydroxymethylation at the *C9ORF72* promoter reported a reduction in 5-methylcytosine (5mC) levels during reprogramming and re-acquiring upon neuronal specification, alongside an increase in 5-hydroxymethylcytosine (5hmC) levels following reprogramming with elevated levels present in iPSCs and MNs (200). However, the use of one patient line and the considerable heterogeneity due to different HRE sizes within and between cellular populations of different developmental stages require cautious interpretation of the results.

Cohen-Hadad et al. assessed DNA methylation at the *C9ORF72* HRE and the upstream 5' CpG island (*C9ORF72* promoter region) in differentiated neural precursors and teratomas derived from *C9ORF72* HRE human embryonic stem cell (hESC) and iPSC lines (219). The 5' CpG and the HRE itself were found to be hypermethylated in the *C9ORF72* HRE iPSC-NPCs and teratomas. Despite the considerable difference in the HRE size between the iPSC and hESC lines, the authors concluded that reprogramming leads to hypermethylation of the *C9ORF72* promoter region in iPSCs which may lead to milder phenotypes in iPSCs compared to ESCs. This is supported by the finding of increased intron 1-retaining *C9ORF72* transcripts in NPCs and teratomas differentiated from *C9ORF72* HRE hESCs compared to iPSCs. The DNA methylation status of the 5' CpG island upstream of the HRE was also assessed in a recent study (207). The authors reported hypermethylation of the 5' CpG island, increased intron 1-retaining *C9ORF72* transcripts as well as a reduction in total, V1 and V2 *C9ORF72* RNA in iPSC-MNs from one patient which were all restored following CRISPR/Cas9 isogenic correction of the *C9ORF72* HRE.

Finally, other major neuropathological hallmarks of C9-FTD/ALS such as p62 inclusions co-localising with DPRs or TDP-43 cytoplasmic mislocalisation and aggregation are not a common finding in *C9ORF72* iPSC models. Some iPSC studies have shown evidence for

elevated p62 levels (197, 199), and p62 cytoplasmic inclusions have been observed under basal conditions (199) and upon chronic sodium arsenite stress (220), however, p62 pathology is not a common finding among iPSC studies. Importantly, even though a nucleocytoplasmic shift of TDP-43 has been reported in iPSC studies (203, 209), the typical cytoplasmic TDP-43 inclusion pathology in C9-FTD/ALS has not been yet recapitulated *in vitro* by iPSC studies under basal conditions. However, it was recently shown that chronic, mild oxidative stress insult by sodium arsenite treatment was able to induce the recruitment of TDP-43 into stress granules as well as the formation of distinct cytoplasmic aggregates of phosphorylated TDP-43 in *C9ORF72* iPSC-MNs (220). Together, these studies show that iPSC-neurons from patients with the *C9ORF72* HRE can recapitulate RNA foci, DPRs and *C9ORF72* haploinsufficiency.

ii) Investigating C9ORF72 function in iPSC neurons

A role of *C9ORF72* protein in endosomal trafficking and autophagy has been suggested (181) and several independent studies have further supported the function of *C9ORF72* in the induction of autophagy (182, 183, 185, 186). *C9ORF72* iPSC studies have confirmed the role of *C9ORF72* protein in autophagy and elucidated novel aspects of *C9ORF72* cellular function. *C9ORF72* patient-derived neurons were found to exhibit elevated levels of the autophagy marker p62 compared to controls (197, 199) reminiscent of the p62 positive/ubiquitin positive/TDP43 negative DPR pathology observed in C9-FTD/ALS patients (221). Compromised autophagy and a reduction in basal autophagy levels have been observed in *C9ORF72* iPSC-neurons (182, 197). Compromised extracellular vesicle secretion and endosome formation as well as dysfunctional trans-Golgi network were also observed in *C9ORF72* HRE MNs by Aoki et al. (189). The *C9ORF72* protein was found to localise in early endosomes and was required for normal vesicle trafficking and lysosomal biogenesis in

iPSC-MNs (212). *C9ORF72* haploinsufficiency could therefore trigger neurodegeneration by causing accumulation of glutamate receptors, leading to MN excitotoxicity, and hypersensitivity of MNs to neurotoxic DPRs by impairing their clearance (212). This could be rescued by restoring *C9ORF72* levels or treatment with small molecule modulators of vesicle trafficking. Finally, Sivadasan et al. provided evidence that *C9ORF72* regulates axonal actin dynamics via regulation of the GTPase activity of Arf6 and the phosphorylation of cofilin, an ubiquitous actin-binding factor required for the reorganization of actin filaments (213).

iii) Novel pathways identified in C9ORF72 iPSC-neurons

Importantly, apart from recapitulating C9-FTD/ALS pathology, a plethora of iPSC studies have shed light on novel disease mechanisms linked to *C9ORF72* HRE. Nucleocytoplasmic transport has been found by several independent groups to be impaired in FTD/ALS linked to *C9ORF72* HRE (209, 222-225). A disrupted nuclear-cytoplasmic pattern for total RNA (222), Ran GTPase-activating protein 1 (RanGAP1) (209, 224), TDP-43 (209), Ran-GEF RCC1 (223), and RNA editing enzyme adenosine deaminase acting on RNA 2 (ADAR2) (225) have been identified in *C9ORF72* HRE neurons.

Several studies have investigated dysregulated cellular processes leading to increased vulnerability *C9ORF72* iPSC-neurons to ER and oxidative stress, mitochondrial dysfunction and excitotoxicity (199, 204-206, 212, 226). Dafinca et al. reported elevated ER calcium levels, reduced mitochondrial membrane potential and reduced levels of the antiapoptotic protein Bcl-2 in *C9ORF72* patient-derived MNs compared to control MNs (199).

Furthermore, *C9ORF72* HRE cortical and MNs displayed increased susceptibility to apoptosis, elevated p62 levels, abnormal protein aggregation and stress granule formation

compared to control neurons. In a follow-up study, Ababneh et al. reported reversal of all HRE-related phenotypes upon CRISPR/Cas9 correction of the HRE in iPSC lines from one patient (207). The phenotypes included susceptibility of *C9ORF72* MNs to apoptosis, increased number of stress granules, HRE-containing intron 1 retention, 5' CpG hypermethylation and reduced *C9ORF72* RNA expression. Several other studies have also shown vulnerability of *C9ORF72* patient-derived neurons to excitotoxicity (204, 206, 212). Lopez-Gonzalez et al. demonstrated that poly-GR led to mitochondrial dysfunction, age-dependent increase in oxidative stress and DNA damage as indicated by an increase in DNA damage marker γ H2AX, in *C9ORF72* patient-derived MNs (205). They also showed that reduction of oxidative stress partially reduced DNA damage in *C9ORF72* patient-derived MNs suggesting that oxidative stress could play an important role in the disease pathogenesis and its reduction has therapeutic potential in C9-FTD/ALS. Additional studies have further implicated the DNA damage response in *C9ORF72* neurodegeneration. Increased DNA damage marker γ H2AX as well as RAL5 – a component of the SSA repair machinery, and phosphorylated RAD52, were found in *C9ORF72* patient-derived MNs (226). CRISPR/Cas9-mediated excision of the HRE resulted in reduction of RAD52 hyperactivation. These findings suggest HRE-mediated DNA damage in patient-derived MNs leads to deficits in homology-directed DNA double strand break (DSB) repair pathways.

Altered axonal trafficking, axonal degeneration and synaptic vesicle recycling have also been observed in *C9ORF72* patient-derived neurons (203, 227, 228). Coyne et al. showed that synaptic vesicle cycling was impaired in *C9ORF72* patient-derived MNs due to posttranscriptional reduction in the levels of the Hsc70-4/HSPA8 chaperone (228). Axonal degeneration and partial TDP-43 translocation to the cytoplasm, reminiscent of the TDP-43 pathology observed in C9-FTD/ALS patients, was observed in *C9ORF72* patient-derived

neurons (203). The authors demonstrated that transcription elongation factor AFF2/FMR2 regulates the transcription of the HRE and CRISPR-Cas9-mediated knockout of AFF2/FMR2 resulted in decreased expression of the mutant *C9ORF72* allele containing the HRE and rescue of axonal degeneration and TDP-43 mislocalisation. Finally, patient-derived MNs exhibited axonal transport defects, as indicated by lysosomal track displacement in distal and proximal axons, compared to control MNs (227). This was accompanied by reduced levels of ubiquitously expressed chaperone HSP70 and altered stress granule formation compared to control MNs. Interestingly, all these phenotypes were exacerbated in isogenic *C9ORF72* patient-derived MNs that contained the HRE as well as a *C9ORF72* knockout, supporting a combination of gain and loss of function mechanisms in C9-ALS/FTD pathogenesis.

Finally, the first *C9ORF72* three dimensional neuronal model revealed re-engagement of cell cycle-associated proteins and a senescence-associated secretory phenotype in *C9ORF72* patient-derived neurons (229). Specifically, *C9ORF72* patient-derived neurons grown on Alvetex scaffold spontaneously re-expressed cyclin D1 12 weeks post-differentiation, suggesting cell cycle re-engagement. *C9ORF72* neurons exhibited increased expression of senescence-associated genes including CXCL8, a chemokine overexpressed by senescent cells. In addition to this, increased levels of components of the senescence-associated secretory phenotype were present in media from *C9ORF72* neurons compared to controls.

iv) Alterations in neuronal function in C9ORF72 iPSC-neurons

Neuronal excitability impairments are frequently observed in *C9ORF72* patients (230), therefore several studies have investigated the electrophysiological properties of *C9ORF72* iPSC-neurons. Two studies have found that *C9ORF72* patient-derived MNs were characterised by hyperexcitability compared to control MNs at 2 to 4 weeks post

differentiation (231, 232). In direct contrast, Sareen et al. reported loss of excitability in 2-month-old *C9ORF72* patient-derived MNs as well as altered expression of genes involved in membrane excitability, including the delayed rectifier potassium channel (KCNQ3) which is consistent with hypoexcitability (198). These conflicting findings between the studies may be attributed to the different developmental stage of the MNs, as indicated by a temporal analysis of *C9ORF72* patient-derived MN excitability (231). Devlin et al. showed that *C9ORF72* patient-derived MNs were characterised by intrinsic hyperexcitability at early time points (3-4 weeks) in culture, followed by progressive loss of action potential output and synaptic activity in MNs reaching 9-10 weeks in culture. Interestingly, the loss of excitability manifests at a similar timepoint during MN differentiation as in the study of Sareen et al. (198). Finally, Selvaraj et al. showed no differences in the excitability of *C9ORF72* patient-derived MNs compared to control MNs and isogenic CRISPR/Cas9 *C9ORF72* HRE-corrected MNs (206). The authors attributed the lack of changes in excitability to the purity of MN cultures, compared to other studies using mixed cultures of MNs and glia, suggesting glia-mediated non-cell-autonomous mechanisms may alter MN function. Indeed, in a follow-up study, Zhao et al. demonstrated that *C9ORF72* patient-derived astrocytes induced progressive loss of action potential output in control iPSC-MNs caused by an underlying loss of voltage activated Na⁺ and K⁺ currents (208).

v) Non-cell-autonomous disease mechanisms in C9ORF72 iPSC-neurons

Patient-derived iPSC models provide an ideal platform to investigate non-cell-autonomous disease mechanisms. To date, several groups have demonstrated a toxic effect of *C9ORF72* patient-derived astrocytes and oligodendrocytes to MNs or other cell types either in co-cultures or via conditioned media. In an early study of non-cell-autonomous toxicity mechanisms in C9-ALS, Meyer et al. showed that *C9ORF72* transdifferentiated human

astrocytes were toxic to co-cultured mouse MNs (233). *C9ORF72* iPSC-astrocytes were shown to modulate the autophagy pathway in a non-cell-autonomous manner (234). Specifically, cells treated with patient-derived astrocyte conditioned medium exhibited reduced expression of the autophagosomal marker LC3-II, with a concomitant accumulation of p62 puncta and increased SOD1 expression. Increased oxidative stress was detected in *C9ORF72* patient-derived astrocytes and *C9ORF72* astrocyte conditioned media was also found to be neurotoxic by inducing oxidative stress in control MNs (235). Varcianna et al. reported dysregulation of extracellular vesicle formation and miRNA cargo in *C9ORF72* induced astrocytes which affected neurite network maintenance and MN survival (236). They identified downregulation of miR-494-3p, a negative regulator of the axon guidance protein semaphorin 3A (SEMA3A), and showed that restoration of miR-494-3p levels can downregulate Sema3A levels in MNs and increase MN survival. *C9ORF72* patient-derived astrocytes recapitulated key pathological features of C9-ALS and caused a progressive loss of action potential output in co-cultured control MNs which was reversed upon CRISPR/Cas-9-mediated excision of the HRE (202). Importantly, these phenotypes were only present in control MNs co-cultured with *C9ORF72* patient-derived astrocytes and not in *C9ORF72* patient-derived MN-enriched cultures alone, providing further evidence for the role of non-cell-autonomous toxicity mechanisms in neurodegeneration. Finally, apart from astrocytes, patient-derived oligodendrocytes have also been shown to induce MN death in both co-cultures and via oligodendrocyte conditioned media (237).

vi) Using C9ORF72 iPSC models for the development of novel therapeutics

Ultimately, the use of iPSCs for the study of *C9ORF72* FTD/ALS pathogenic mechanisms is aimed at the development of novel therapies. Two independent studies have provided evidence for the therapeutic potential of antisense oligonucleotides (ASOs) in C9-FTD/ALS

which are currently being tested in *C9ORF72* HRE patients (<https://clinicaltrials.gov/ct2/show/study/NCT03626012>) (198, 204). Donnelly et al. reported sequestration of RNA editing regulator ADARB2 by the *C9ORF72* HRE expanded RNA, aberrant gene expression and susceptibility to glutamate excitotoxicity in *C9ORF72* HRE mixed neurons compared to controls (204). In the second ASO study by Sareen et al. the *C9ORF72* patient-derived MNs exhibited RNA foci that co-localised with RNA-binding proteins hnRNPA1 and Pur- α , as well as aberrant gene expression, and reduced excitability compared to control MNs (198). In both studies the use of ASOs targeting the *C9ORF72* transcript resulted in reversal of the toxicity phenotypes in patient-derived neurons. Furthermore, as the ASO-mediated *C9ORF72* knockdown had no adverse effect on patient-derived neurons, the authors argued against a loss of function mechanism as the major pathogenic cause of C9-FTD/ALS. However, recent studies have elucidated the important function of *C9ORF72* in autophagy and provided evidence for a contribution of *C9ORF72* haploinsufficiency in FTD/ALS pathogenesis, proposing the use of ASOs that do not reduce *C9ORF72* expression. Interestingly, the use of ASOs restored the impaired nucleocytoplasmic transport phenotype that was responsible for the abnormal nuclear/cytoplasmic ratios of Ran and TDP-43 in another study of *C9ORF72* HRE neurons (209). Collectively, the ASO intervention studies in human *C9ORF72* iPSC neurons have shown that specific targeting of the *C9ORF72* transcript can rescue gain of function toxicity and has therapeutic value. Using small molecules that bind and specifically stabilise the *C9ORF72* HRE G-quadruplex RNA, Simone et al. demonstrated a reduction in RNA foci burden in both *C9ORF72* HRE cortical neurons and MNs as well as a reduction in the levels of poly-GP in *C9ORF72* HRE MNs (202). These data provide proof of principle that targeting the *C9ORF72* HRE G-quadruplex structure has therapeutic potential. Finally, in a phenotypic screen to repurpose existing drugs, Imamura et al. identified the Src/c-Abl

pathway as a novel potential therapeutic target in ALS, and Bosutinib, a Src/c-Abl inhibitor, was shown to increase survival of *C9ORF72* patient-derived MNs (238).

iPSC models of *TARDBP* mutations

Bilican et al. differentiated clonal iPSC lines from two controls and an ALS patient with a *TARDBP* M337V mutation into MNs (239). They noted higher levels of soluble and detergent-resistant TDP-43 in M337V MNs, despite apparently normal levels of nuclear TDP-43. They found higher levels of C-terminal TDP-43 fragments in the insoluble fraction and higher levels of full-length TDP-43 in the soluble fraction. M337V MNs had reduced cell viability and an increased sensitivity to a PI3K inhibitor (LY294002), although no differences in the response to a MAPK inhibitor (U0126) or an endoplasmic reticulum stressor (thapsigargin) were observed. The same iPSC lines were used by Serio et al. to generate astrocytes (240). The astrocytes had similar phenotypes to the MNs including mis-localised, cytoplasmic TDP-43, increased levels of soluble TDP-43 and reduced viability. The authors suggested that the increased TDP-43 levels are likely due to the mutation resulting in PTMs that increase TDP-43 stability and/or slow its clearance. In contrast to the MNs, they found no difference in detergent-resistant, insoluble TDP-43, indicating that the mutation has distinct cell type specific effects. Co-culture of MNs with either control or M337V astrocytes resulted in improved viability, showing that M337V astrocytes do not exert a toxic effect on MNs, unlike what has previously been observed in SOD1-linked ALS (241).

Zhang et al. differentiated iPSC lines from an FTD/ALS patient with *TARDBP* A90V mutation, an unaffected family member with no known disease-causing mutations, and the M337V iPSC line previously used in the Bilican et al. study into neurons (106, 239).

Treatment with the broad-spectrum kinase inhibitor staurosporine resulted in cytoplasmic

mislocalisation of TDP-43 in both control and patient lines, but with a higher ratio of cytoplasmic: nuclear TDP-43, lower levels of total TDP-43 and higher rates of neuronal death in the patient neurons. They also identified decreased levels of the neuroprotective miR-9 and its precursor (miR-9-2) in the patient-derived neurons. They did not find differences in TDP-43 profile between the control and patient iPSC-neurons under control conditions or in response to other stressors. Bossolasco et al. also did not find any significant increase in cytoplasmically mislocalised TDP-43 in neurons with the A382T mutation (242) under control conditions.

Multiple studies have also shown the potential of iPSCs from patients with *TARDBP* mutations as a suitable model for drug screening. Egawa et al. found cytoplasmically mislocalised, aggregated TDP-43 and shorter neurites in iPSC-MNs from ALS patients with *TARDBP* (Q343R/ M337 V/G298S) mutations (243). It is not clear if this identification of aggregates, which were either not detected or not mentioned in the previous studies using iPSCs with M337V mutations, was due to differentiation to a particular cell-type or differences in detection methods. Katti et al. did find stress granules and phosphorylated TDP-43 aggregates in *TARDBP* iPSC-MNs after inducing stress through sodium arsenite treatment, whereas there were only very low levels of phosphorylated TDP-43 under control conditions (220). This suggests that stress might be necessary to induce TDP-43 pathology in iPSC-derived neurons and might explain differences in TDP-43 observations between studies. In the patients MNs, Egawa et al. found the spliceosomal factor SNRNP2 bound to TDP-43, which could be rescued by the histone acetyltransferase inhibitor, anacardic acid. Another study found abnormalities in mitochondria, lysosomes and axonal trafficking in G294V neurons, the latter was rescued by treating with the osmolyte D-sorbitol (244). Burkhardt et al. developed a screen using iPSC-MNs from sporadic and familial ALS

patients, including a patient with a *TARDBP* mutation and found hyper-phosphorylated TDP-43 aggregates in neurons from the sporadic ALS patients but did not detect aggregates in control neurons or neurons from the *TARDBP* A315T patient. They identified compounds that reduced TDP-43 aggregation in patient neurons. They also detected higher levels of TDP-43 in MNs but did not find higher levels in the sporadic ALS neurons with aggregates (245). Yang et al. used iPSC-neurons further validate the treatment potential of Kenpaullone, a multikinase inhibitor that had been found to increase neuronal survival in mutant *SOD1* mouse embryonic stem cells (246). Together, these studies show that iPSC-neurons with mutations in *TARDBP* can recapitulate key aspects of TDP-43 pathology (Figure 5), although they may not display all of the phenotypes seen in *TARDBP* mutation patients, and that they can be used to identify or validate promising treatment options.

Summary and Future Directions

The generation of iPSCs from patients with phenotypes/genotypes of interest and their subsequent differentiation into homogeneous populations of specific cell types has enabled the development of patient-specific *in vitro* models of familial FTD (Figure 1). This approach has been successfully used in an ever-increasing number of studies to model the most common genetic causes of FTD and FTD-ALS. In spite of this early success, several challenges still remain. The advantages and limitations of using iPSC-derived cells to model FTD have been summarised in Table 5.

On a technical level, the cost of iPSC work can be prohibitive, and restricts the number of patient and control lines that can be used in a single study. Although iPSC-neurons do present with some key markers of FTD, for example increased tau phosphorylation and tau mislocalisation in FTD with *MAPT* mutations (Figure 2), progranulin haploinsufficiency in FTD with *GRN* mutations, (Figure 3) and TDP-43 mislocalisation in FTD with *GRN* or

TARDBP mutations (Figures 3 and 5), these models do not recapitulate the full pathologies observed in FTD patients. For example, iPSC- neurons with *MAPT* mutations, do not show neurofibrillary tangles, only occasional accumulations of insoluble phosphorylated or misfolded tau species (67, 247) and studies using iPSC-neurons with *GRN* and *TARDBP* mutations do not always find TDP-43 aggregation, mislocalisation or increased levels of insoluble TDP-43 (Tables 2 and 4). Similarly, although *C9ORF72* iPSC studies have successfully recapitulated C9-FTD/ALS pathology associated with RNA foci and DPRs, they do not develop robust TDP-43 pathology, only early-stage TDP-43 mislocalisation, unless chronic stress is applied in neuronal cultures (220). Multiple transcriptomics studies have demonstrated that iPSC-neurons are fetal in nature (63, 64), which presents a challenge when investigating age-related neurodegenerative diseases such as FTD. Induction of age-associated phenotypes to increase the physiological relevance of iPSC-derived models could be explored, for example, introducing reactive oxidative stress, DNA damage and mitochondrial damage, traits typically associated with aged cells (248). Telomerase inhibitors (249) and progerin, a derivative of lamin A associated with premature ageing, (250) have been used to induce age-associated phenotypes, such as accumulation of ROS and DNA damage and shorter dendrites in iPSC-neurons.

Inter and intra-patient variability in iPSCs, linked to genetic heterogeneity, is a known challenge of working with human iPSCs (251), and the generation of isogenic controls by gene-editing may help to control this issue (252). However, understanding the contribution of gene modifiers to cellular phenotypes is an important question: for example, *TMEM106B* variants can modify the phenotype of both *GRN* and *C9ORF72* mutation carriers (253-255) and the protective variant has been shown to ameliorate lysosomal phenotypes *in vitro* (256). Most studies discussed here did not mention the *TMEM106B* genotype of the cell lines used.

Further, the genetic and neuropathological overlap between FTD and ALS due to *C9ORF72* repeat expansions and TDP-43 pathology respectively, means that most studies have used either cortical or MNs, and we must exercise caution when extrapolating results from one to other. Future studies to examine neuronal subtype-specific effects, in cells from deeply-phenotyped patients with either ALS or FTD will help us understand the selective vulnerability of these cell types. It should be noted that the majority of studies have generated and analysed only one iPSC-derived neural cell type, such as neurons. It will again be important to understand the contribution of astrocytes and microglia to FTD, and the cross-talk between these cell types in complex, co-culture models. Increased optimisation of 3D cell culture, whereby astrocytes and microglia are infused into neuronal organoids may help us explore cellular crosstalk in FTD (257). However using organoids to model neurodegeneration comes with its own merits and limitations. Whilst organoids are advantageous in that they better replicate the complex structural architecture of the brain compared to 2D models, a lack of tissue maturity and vascularisation limit their usefulness (258). To date, the majority of research using organoids to model neurodegeneration has been focused on Alzheimer's disease (257, 259, 260), however it will be interesting to see how 3D models are used to research FTD and ALS as organoid protocols and molecular techniques continue to improve.

In spite of the aforementioned challenges, iPSC models have given unique insights into disease mechanisms of *MAPT*, *GRN*, *C9ORF72* and *TARDBP* mutations, and provide a novel, physiologically relevant model for drug screening. As future work addresses the challenges outlined above, these patient-derived models will continue to give us unique insights into the molecular mechanisms underpinning neurodegeneration in FTD.

Figure Legends

Figure 1. An overview of iPSC technology

Somatic cells (such as fibroblasts or PBMCs) can be obtained from patients with genotypes/phenotypes of interest and reprogrammed into iPSCs via the exogenous expression of the transcription factors Oct4, Klf4, Sox2 and cMyc. iPSCs can then be differentiated into multiple cell types affected in FTD, which in turn can be used for disease modeling, drug screening and *in vivo* chimeric disease modeling. Somatic cells can also be directly converted into neurons via transdifferentiation.

Figure 2. Common phenotypes observed iPSC-neurons with *MAPT* mutations

A schematic representation displaying common phenotypes observed in iPSC-cortical neurons with *MAPT* mutations, including nuclear invaginations and folds, increased tau phosphorylation, accumulation of misfolded tau, increased electrophysiological activity, increased 4R:3R tau ratio, increased tau fragmentation, decreased neurite length, and increased reactive oxygen species

Figure 3. Common phenotypes observed iPSC-neurons with *GRN* mutations

A schematic representation displaying common phenotypes observed in iPSC-cortical neurons with *GRN* mutations. These include; reduced intracellular and extracellular progranulin protein, reduced *GRN* mRNA, reduced nuclear TDP-43, increased insoluble and cytoplasmic TDP-43, impaired lysosomal function, reduced Cathepsin D activity, reduced miR-124 and increased expression of GluA2 and GluA4 AMPAR subunits. Deficits in WNT signaling, PI3K/AKT pathways and MEK/MAPK pathways have also been identified, as well as the cleavage of progranulin into individual granulins by cathepsin L at the lysosome.

Figure 4. Common phenotypes observed iPSC-neurons with *C9ORF72* mutations

A schematic representation displaying common phenotypes observed in iPSC-neurons from patients carrying the *C9ORF72* HRE including intranuclear RNA foci that sequester RNA-binding proteins, DNA damage, nucleocytoplasmic transport defects, DPR aggregates, vulnerability to ER stress and excitotoxicity, mitochondrial dysfunction, compromised autophagy, lysosomal dysfunction and impaired excitability. Non-cell-autonomous toxicity from patient-derived astrocytes and oligodendrocytes has also been demonstrated.

Figure 5. Common phenotypes observed iPSC-neurons with *TARDBP* mutations

A schematic representation displaying phenotypes observed in iPSC-cortical neurons with *TARDBP* mutations. These include; increased insoluble and cytoplasmic TDP-43, TDP-43 aggregation, shorter neurites, shrunken lysosomes, reduced miR-9 and pre miR-9-2, initial hyperexcitability followed by a loss of electrophysiological signal, neurofilament abnormalities and abnormal trafficking of organelles.

Acknowledgements

EP and SW are supported by the National Institute for Health Research University College London Hospitals Biomedical Research Centre. SW is supported by an Alzheimer's Research UK Senior Research Fellowship (ARUK-SRF2016B-2).GL is supported by a BBSRC CASE studentship and JC is supported by the EPSRC. We apologise to colleagues whose work has been omitted due to space constraints.

Table 1 : Summary of phenotypes identified in studies using *MAPT* mutation iPSC-neurons

<i>Gene</i> (<i>Mutation</i>)	<i>Referenc</i> <i>e</i>	<i>Cell</i> <i>type</i>	<i>Phenotype</i>				
			↑ 4R tau	↑ Tau phosphorylato n	Tau mis- localisatio n	Accumulatio n of misfolded, insoluble or aggregated tau species	Additional observations
<i>MAPT</i> (10+16)	Sposito et al., (2015). (65)	Cortical neurons	Y	N	N/A	N/A	<ul style="list-style-type: none"> Neurons in extended culture up to 365 days expressed all 6 tau isoforms
	Paonessa et al., (2019). (70)	Cortical neurons	Y	Y	Y	N	<ul style="list-style-type: none"> Mislocalization of tau from axons to cell body and dendrites Nuclei were more frequently seen with folds and invaginations Defective nucleocytoplasm

							mic transport
<i>MAPT</i> (10+14)	Imamura et al., (2016). (82)	Cortical neurons	Y	N/A	N/A	Y	<ul style="list-style-type: none"> • Sensitivity to electrical stimulation, invoking a larger calcium release compared to controls • Inhibition of calcium influx decreased intracellular and extracellular mis-folded tau, and increased cell survival
<i>MAPT</i> (P301L)	Iovino et al., (2015). (67)	Cortical neurons	N	Y	N	N	<ul style="list-style-type: none"> • Earlier electrophysiological maturation and altered mitochondrial transport compared to controls • Contorted processes with varicosity like

							<p>structures, some containing both alpha-synuclein and 4R tau</p> <ul style="list-style-type: none"> • Tau localised in cell bodies in both mutant and control cells
MAPT (N279K)	Wren et al., (2015). (85)	NSC	Y	N/A	N/A	N/A	<ul style="list-style-type: none"> • Increased stress granules and impaired lysosomal trafficking
	Ehrlich et al., (2015). (84)	Mixed neurons	Y	Y	N	N	<ul style="list-style-type: none"> • Increased tau fragmentation • Increased vulnerability to oxidative and ER stress • Decreased neurite length
MAPT (N279K)	Iovino et al., (2015). (67)	Cortical neurons	Y	Y	N	Y	<ul style="list-style-type: none"> • Earlier electrophysiological maturation • Decreased anterograde mitochondrial

							transport <ul style="list-style-type: none"> • Tau localised in cell bodies in both mutant and control cells
<i>MAPT</i> (A152T)	Fong et al., (2013). (261)	Mixed neurons	N/A	Y	Y	N/A	<ul style="list-style-type: none"> • Punctate tau • Short neurites with bulges, constrictions and odd bends, axonal degeneration
	Silva et al., (2016). (107)	Cortical neurons	N/A	Y	Y	Y	<ul style="list-style-type: none"> • Accumulation of insoluble phosphorylated tau • Increased autophagy and UPS markers, suggesting proteostasis impairment
<i>MAPT</i> (V337M)	Ehrlich et al., (2015). (84)	Mixed neurons	N	Y	N	N	<ul style="list-style-type: none"> • Increased tau fragmentation • Decreased neurite length

							<ul style="list-style-type: none"> • Increased vulnerability to cell stress
<i>MAPT</i> (R406W)	Imamura et al., (2016). (82)	Cortical neurons	N/A	N/A	N/A	Y	<ul style="list-style-type: none"> • Sensitivity to electrical stimulation, invoking a larger calcium release compared to controls • Inhibition of calcium influx decreased intracellular and extracellular misfolded tau, and increased cell survival
<i>MAPT</i> (10+16 , P301L and N279K triple mutant)	Garcia-Leon et al., (2018). (91)	Cortical neurons	Y	N	Y	Y*	<ul style="list-style-type: none"> • *Endogenously triggered tau aggregation • Increased electrophysiological activity • Decreased neurite outgrowth <p>Significant</p>

							activation of stress response pathways
--	--	--	--	--	--	--	--

Table 2: Summary of phenotypes identified in studies using *GRN* mutation iPSC derived cells

<i>Gene (Mutation)</i>	<i>Reference</i>	<i>Cell type</i>	<i>Phenotype</i>			
			Progranulin haploinsufficiency	Mislocalised TDP-43	↑ Insoluble TDP-43 or TDP-43 aggregates	Additional observations
<i>GRN</i> (S116X)	Almeida et al., (2012). (156)	Mixed neurons and microglia	Y	Y	N/A	<ul style="list-style-type: none"> Deficits in PI3K/AKT and MEK/MAPK pathways (rescued by increasing progranulin expression)

<i>GRN</i> (S116X) & <i>C9ORF72</i> HRE	Gascon et al., (2014). (159)	Mixed neurons	N/A	N/A	N/A	<ul style="list-style-type: none"> Decreased miR-124 Increased expression of GluA2 and GluA4 AMPAR subunits
<i>GRN</i> (S116X)	Lee et al., (2014). (158)	Mixed neurons	Y	N/A	N/A	<ul style="list-style-type: none"> Increased progranulin levels, following inhibition of SORT1 endocytosis
<i>GRN</i> (S116X)	Almeida et al., (2016). (160)	Cortical neurons	Y	N/A	N/A	<ul style="list-style-type: none"> Increased progranulin after suberoylanilide hydroxamic acid (a histone deacetylase inhibitor)

<i>GRN</i> (S116X)	Lee et al., (2017). (161)	Mixed neurons	N/A	N/A	N/A	<ul style="list-style-type: none"> • Cathepsin L cleaves progranulin into individual granulins in the lysosome
<i>GRN</i> (IVS1+5G>C)	Raitano et al., (2015). (171)	Cortical and motor neurons	Y	N	N	<ul style="list-style-type: none"> • Decreased corticogenesis • Deficits in WNT signalling • Altered gene expression
<i>GRN</i> (R198GfsX19)	Holler et al., (2016). (163)	Mixed neurons	Y	N/A	N/A	<ul style="list-style-type: none"> • <i>GRN</i> mRNA haploinsufficiency in fibroblasts • Trehalose increased progranulin in patient -derived neurons
<i>GRN</i> (c.26C>A, p.A9D)	Valdez et al., (2017). (151)	Cortical neurons	Y	Y	Y	<ul style="list-style-type: none"> • Decreased cathepsin D activity, specifically due to granulin E • Lysosomal dysfunction • Isogenic control line: rescued phenotype

Journal Pre-proof

Table 3: Summary of phenotypes identified in studies using *C9ORF72* iPSC-neurons

<i>Gene</i> (<i>Mutation</i>)	<i>Reference</i>	<i>Cell type</i>	<i>Phenotype</i>			
			RNA foci	DPRs	Reduced <i>C9ORF72</i> expression	Additional observations
<i>C9ORF72</i> (<i>GGGGCC</i>) _n	Almeida et al., (2013). (197)	Cortical neurons	Y	Y	Y	<ul style="list-style-type: none"> Increased p62 Compromised autophagy
	Donnelly et al., (2013). (204)	Mixed neurons		Y	Y	<ul style="list-style-type: none"> Sequestration of RNA binding proteins by the expanded RNA Validation of ADARB2 interaction Aberrant gene expression Susceptibility to glutamate excitotoxicity
	Sareen et al., (2013). (198)	Motor neurons	Y	N	N	<ul style="list-style-type: none"> RNA foci colocalisation with hnRNPA1 and Pur-α Aberrant gene expression Reduced excitability
	Meyer et al., (2014). (233)	Induced astrocytes	N/A	N/A	N/A	<ul style="list-style-type: none"> Non cell autonomous toxicity of induced astrocytes to co-cultured mouse MNs

	Wainger et al., (2014). (232)	Motor neurons	N/A	N/A	N/A	<ul style="list-style-type: none"> • Hyperexcitability • Kv7 channel activator retigabine blocked the hyperexcitability
	Devlin et al., (2015). (231)	Motor neurons	Y	N/A	N/A	<ul style="list-style-type: none"> • No changes in cell viability • Initial hyperexcitability followed by a progressive loss in action potential output and synaptic activity
	Zhang et al., (2015). (209)	Motor neurons	Y	N/A	N/A	<ul style="list-style-type: none"> • Mislocalisation of RanGAP1 and interaction with HRE RNA • Disrupted nuclear-cytoplasmic pattern of Ran • RanGAP1 overexpression rescued Ran pattern • Abnormal nuclear/cytoplasmic ratio of TDP-43 • Impaired nucleocytoplasmic transport
	Freibaum et al., (2015).	Cortical neurons	N/A	N/A	N/A	<ul style="list-style-type: none"> • RNA nuclear export defect, retention of RNA

(222)						<p>in nuclei</p> <ul style="list-style-type: none"> • ~ 35% increase in the nuclear/cytoplasmic ratio of RNA density
Jovicic et al., (2015). (223)	Induced neurons	N/A	N/A	N/A		<ul style="list-style-type: none"> • Reduction in nuclear localization of RCC1
Esanov et al., (2016). (200)	Motor neurons	N/A	N/A	N/A		<ul style="list-style-type: none"> • Reduced 5mC levels (methylation) in <i>C9ORF72</i> promoter during reprogramming and re-acquiring upon neuronal specification • Increased 5hmC levels (hydroxymethylation) in <i>C9ORF72</i> promoter in iPSCs and MNs
Cohen-Hadad et al., (2016). (219)	NPCs, teratomas	N/A	N/A	N		<ul style="list-style-type: none"> • <i>C9ORF72</i> promoter hypermethylated in <i>C9ORF72</i> HRE iPSC lines but unmethylated in <i>C9ORF72</i> HRE ESCs • Increased levels of intron 1-retaining <i>C9ORF72</i> transcripts in NPCs and teratomas from <i>C9ORF72</i> HRE ESCs compared to those derived from iPSCs
Dafinca et	Cortical neurons,	Y	Y	N/A		<ul style="list-style-type: none"> • Increased ER calcium

	al., (2016). (199)	Motor neurons				<p>levels</p> <ul style="list-style-type: none"> • Reduced mitochondrial membrane potential • Reduced levels of the anti-apoptotic protein Bcl-2 • Increased susceptibility to apoptosis • Elevated p62 levels • Abnormal protein aggregation and stress granule formation
	Westergard et al., (2016). (211)	Motor neurons	N/A	Y	N/A	<ul style="list-style-type: none"> • Cell-to-cell transmission of DPRs • Transmission of poly-GA and poly-GR aggregates but not poly-GP from <i>C9ORF72</i> to control MNs in both co-culture and via conditioned media
	Ferraiuolo et al., (2016). (237)	Oligodendrocytes	N/A	N/A	N/A	<ul style="list-style-type: none"> • Patient-derived oligodendrocytes induced MN death in both co-cultures and via oligodendrocyte conditioned media
	Lopez-Gonzalez et	Motor neurons	Y	Y	N/A	<ul style="list-style-type: none"> • Mitochondrial dysfunction

	al., (2016). (205)					<ul style="list-style-type: none"> • Age-dependent increase in oxidative stress and DNA damage • Toxicity caused by poly-GR
	Sivadasan et al., (2016). (213)	Motor neurons	N/A	N/A	Y	<ul style="list-style-type: none"> • Increased phosphorylation of cofilin in <i>C9ORF72</i>-depleted MNs of patients vs controls • <i>C9ORF72</i> modulated activity of small GTPases Arf6 and Rac1, resulting in increased activity of LIM-kinases 1 and 2 (LIMK1/2) and reduced axonal actin dynamics in <i>C9ORF72</i>-depleted patient MNs • Dominant negative Arf6 reversed phenotype suggesting <i>C9ORF72</i> acts as a modulator of small GTPases to regulate axonal actin dynamics
	Aoki et al., (2017). (189)	Motor neurons	N/A	N/A	Y	<ul style="list-style-type: none"> • Deficits in extracellular vesicle secretion, endosome formation and trans-Golgi network

Imamura et al., (2017). (238)	Motor neurons	N/A	N/A	N/A	<ul style="list-style-type: none"> Increased survival in <i>C9ORF72</i> MNs following treatment with bosutinib, a Src/c-Abl inhibitor
Coyne et al., (2017). (228)	Motor neurons	N/A	N/A	N/A	<ul style="list-style-type: none"> Impaired synaptic vesicle cycling due to posttranscriptional reduction in the levels of the Hsc70-4/HSPA8 chaperone HSPA8 levels were reduced in the soma and dendrites of <i>C9ORF72</i> MNs by 57% and 32%, respectively
Simone et al., (2018). (202)	Cortical neurons, Motor neurons	Y	Y	N/A	<ul style="list-style-type: none"> Reduction in RNA foci (CNs and MNs) and poly-GP levels (MNs) following treatment with small molecules that bind <i>C9ORF72</i> HRE G-quadruplex RNA
Selvaraj et al., (2018). (206)	Motor neurons	Y	Y	N	<ul style="list-style-type: none"> No difference in excitability Increased GluA1 AMPAR expression leading to enhanced vulnerability to excitotoxicity

						<ul style="list-style-type: none"> Excision of the HRE resulted in reversal of RNA foci and vulnerability to excitotoxicity phenotypes
	Shi et al., (2018). (212)	Motor neurons	N/A	N/A	Y	<ul style="list-style-type: none"> Reduced survival of patient-derived MNs Interaction of C9ORF72 with endosomes C9ORF72 was required for normal vesicle trafficking and lysosomal biogenesis in MNs Low C9ORF72 activity sensitised MNs to glutamate and DPR toxicity suggesting a synergistic effect between gain and loss of function mechanisms C9ORF72 restoration, constitutively active RAB5 or small molecule modulators of vesicle trafficking all rescued patient MN

						survival
Moore et al., (2019). (225)	Motor neurons	N/A	N/A	N/A		<ul style="list-style-type: none"> Mislocalisation of RNA editing enzyme adenosine deaminase acting on RNA 2 (ADAR2) to the cytoplasm
Cheng et al., (2019). (224)	Motor neurons	N A	Y	N/A		<ul style="list-style-type: none"> Glutamate-induced excitotoxicity Disrupted Ran gradient and nucleocytoplasmic transport Increased RNA helicase DDX3X levels led to reduction in DPRs, rescuing <i>C9ORF72</i> HRE phenotypes of glutamate-induced excitotoxicity and disrupted nucleocytoplasmic transport
Yuva-Aydemir et al., (2019). (203)	Cortical neurons	Y	Y	N/A		<ul style="list-style-type: none"> Axonal degeneration Partially cytoplasmic TDP-43 Transcription elongation factor AFF2/FMR2 regulates the transcription of the HRE

						<ul style="list-style-type: none"> AFF2 knockout resulted in decreased expression of the <i>C9ORF72</i> allele containing the HRE, rescue of axonal degeneration and TDP-43 mislocalisation
	Birger et al., (2019). (235)	Astrocytes	N/A	N/A	N/A	<ul style="list-style-type: none"> Increased oxidative stress <i>C9ORF72</i> astrocyte conditioned media was neurotoxic by inducing oxidative stress in control MNs
	Zhao et al., (2020). (208)	Astrocytes	Y	Y	N	<ul style="list-style-type: none"> Cell-autonomous astrocyte pathology reversed upon CRISPR/Cas-9-mediated excision of the HRE Progressive loss of action potential output in co-cultured control MNs which was reversed upon CRISPR/Cas-9-mediated excision of the HRE Phenotypes only present in control MNs co-cultured with <i>C9ORF72</i> patient-derived astrocytes and not in

						<i>C9ORF72</i> patient-derived MN-enriched cultures alone (non-cell-autonomous mechanisms)
Andrade et al., (2020). (226)	Motor neurons	N/A	N/A	N/A		<ul style="list-style-type: none"> • Increased DNA damage marker γH2AX • Increased RAD5 (component of the SSA repair machinery) and phosphorylated RAD52 • CRISPR/Cas-9-mediated excision of the HRE resulted in reduction of RAD52 hyperactivation
Abo-Rady et al., (2020). (227)	Motor neurons	N/A	Y	N/A		<ul style="list-style-type: none"> • Axonal transport defects • Reduced levels of ubiquitously expressed chaperone HSP70 • Altered stress granule formation • Phenotypes were exacerbated in isogenic <i>C9ORF72</i> patient-derived MNs that contained the HRE as well as a <i>C9ORF72</i> knockout, supporting a combination of gain and loss of function

						mechanisms in C9-ALS/FTD pathogenesis
Porterfield et al., (2020). (229)	Cortical neurons 3D	N/A	N/A	N/A		<ul style="list-style-type: none"> • Spontaneous re-expression of cyclin D1 at 12 weeks post-differentiation, suggesting cell cycle re-engagement • Increased expression of senescence-associated genes including CXCL8, a chemokine overexpressed by senescent cells • Increased levels of components of the senescence-associated secretory phenotype were present in media from <i>C9ORF72</i> neurons
Ababneh et al., (2020). (207)	Motor neurons	Y	Y	N		<ul style="list-style-type: none"> • 5' CpG island hypermethylation in <i>C9ORF72</i> MNs • Retention of the HRE-containing intron in <i>C9ORF72</i> MNs • Susceptibility of in <i>C9ORF72</i> MNs to apoptotic cell death and

						<p>toxicity</p> <ul style="list-style-type: none"> • Reversal of all pathological phenotypes and restoration of <i>C9ORF72</i> expression and methylation levels upon CRISPR/Cas9-mediated excision of the HRE in isogenic MNs
	Ratti et al., (2020). (220)	Motor neurons	N/A	N/A	N/A	<ul style="list-style-type: none"> • Chronic sodium arsenite treatment induced recruitment of TDP-43 into stress granules, formation of distinct cytoplasmic inclusions of phosphorylated TDP-43 and p62 aggregates in <i>C9ORF72</i> MNs

Table 4: Summary of phenotypes identified in studies using *TARDBP* mutation iPSC-neurons and astrocytes

<i>Gene</i> (<i>Mutation</i>)	<i>Reference</i>	<i>Cell type</i>	<i>Phenotype</i>			
			Aggregated TDP-43	Mislocalised TDP-43	↑ Insoluble TDP-43	Additional observations
<i>TARDBP</i> (M337V)	Bilican et al., (2012). (239)	Motor neurons and caudalised neurons	N/A	Y	Y	<ul style="list-style-type: none"> Increased total TDP-43 Decreased survival of patient MNs Increased sensitivity to PI3K inhibitors
<i>TARDBP</i> (M337V)	Serio et al., (2013). (240)	Astrocytes	N	Y	N	<ul style="list-style-type: none"> Increased soluble TDP-43
<i>TARDBP</i> (M337V & A90V)	Zhang et al., (2013). (106)	Mixed neurons	N/A	N	N	<ul style="list-style-type: none"> Decreased total TDP-43 in A90V neurons Increased TDP-43 mislocalisation in patient lines following staurosporine treatment.
<i>TARDBP</i>	Egawa et	Motor	Y	Y	Y	<ul style="list-style-type: none"> TDP-43 binding

(M337V, Q343R and G298S)	al., (2012). (243)	neurons				<p>with SNRPB2 (a spliceosomal factor)</p> <ul style="list-style-type: none"> • Shorter neurites • Phenotype rescued with anacardic acid (a histone acetyltransferase inhibitor)
<i>TARDBP</i> (A315T)	Burkhardt et al., (2013). (245)	Motor and cortical neurons	N	N/A	N/A	<ul style="list-style-type: none"> • Increased levels of TDP-43 and • Detected TDP-43 aggregates in MNs from sporadic ALS patients • Decreased aggregation following treatment with; cyclin-dependent kinase inhibitors, c-Jun N-terminal kinase inhibitors (JNK), Triptolide and FDA- approved cardiac glycosides, Digoxin, Lanatoside C, and Proscillaridin A
<i>TARDBP</i>	Yang et al.,	Motor	N/A	N/A	N/A	<ul style="list-style-type: none"> • Decreased survival

(M337V)	(2013). (246)	neurons				of patient MNs <ul style="list-style-type: none"> Kenpaullone (a multikinase inhibitor) significantly improved MN survival
<i>TARDBP</i> (M337V) & <i>C9ORF72</i> HRE	Devlin et al., (2015). (231)	Motor neurons	N/A	N/A	N/A	<ul style="list-style-type: none"> Initial hyperexcitability followed by progressive loss of action potential output and synaptic activity No changes in cell viability
<i>TARDBP</i> (A382T)	Bossolasco et al., (2018). (242)	Motor neurons	N	N	N/A	<ul style="list-style-type: none"> No difference in TDP-43 levels, compared to controls
<i>TARDBP</i> (S393L and G294V)	Kreiter et al., (2018). (244)	Motor neurons	N	N	N/A	<ul style="list-style-type: none"> Abnormal trafficking, mitochondria and lysosomes (D-sorbitol rescued trafficking deficits) Decreased survival of patient MNs

Table 5: Advantages and limitations of using iPSC- derived cells to model FTD.

Advantages	Limitations
<ul style="list-style-type: none"> • Production of disease relevant and species-specific cell types. • Endogenous expression of mutant genes of interest. • Expansive resources of iPSCs with a range of FTD mutations available • Range of accessible protocols that yield a high volume of cells which is beneficial for screening assays. • Induction of iPSCs into neurons is developmentally comparable to in vivo neurogenesis. • Models have been shown to reflect select number of phenotypes present in patients. • The ability to investigate cellular mechanisms in iPSC derived models alongside tracking patient progress from which the iPSCs were derived. 	<ul style="list-style-type: none"> • Inter and intra variability in iPSCs linked to genetic heterogeneity • iPSC derived models do not recapitulate all phenotypes observed in disease • Often only looking at a single cell type which limits biological relevance. • Cost of iPSC culture, and the time it takes to acquire cells may be prohibitive. • iPSC-neurons are fetal in nature which poses problems for investigating diseases associated with aging.

References

1. Le Ber I, Camuzat A, Guerreiro R, Bouya-Ahmed K, Bras J, Nicolas G, et al. SQSTM1 mutations in French patients with frontotemporal dementia or frontotemporal dementia with amyotrophic lateral sclerosis. *JAMA neurology*. 2013;70(11):1403-10.
2. Bott NT, Radke A, Stephens ML, Kramer JH. Frontotemporal dementia: diagnosis, deficits and management. *Neurodegener Dis Manag*. 2014 4(6):439-54.
3. Chow TW, Miller BL, Hayashi VN, Geschwind DH. Inheritance of frontotemporal dementia. *Arch Neurol*. 1999;56(7):817-22.
4. Rohrer JD, Guerreiro R, Vandrovicova J, Uphill J, Reiman D, Beck J, et al. The heritability and genetics of frontotemporal lobar degeneration. *Neurology*. 2009;73(18):1451-6.
5. Greaves CV, Rohrer JD. An update on genetic frontotemporal dementia. *J Neurol*. 2019;266(8):2075-86.
6. Clark LN, Poorkaj P, Wszolek Z, Geschwind DH, Nasreddine ZS, Miller B, et al. Pathogenic implications of mutations in the tau gene in pallido-ponto-nigral degeneration and related neurodegenerative disorders linked to chromosome 17. *Proc Natl Acad Sci U S A*. 1998;95(22):13103-7.
7. Hutton M, Lendon CL, Rizzu F, Baker M, Froelich S, Houlden H, et al. Association of missense and 5'-splice-site mutations in tau with the inherited dementia FTDP-17. *Nature*. 1998;393(6686):702-5.
8. Poorkaj P, Bird TD, Wijman E, Nemens E, Garruto RM, Anderson L, et al. Tau is a candidate gene for chromosome 17 frontotemporal dementia. *Ann Neurol*. 1998;43(6):815-25.
9. Spillantini MG, Murrell JR, Goedert M, Farlow MR, Klug A, Ghetti B. Mutation in the tau gene in familial multiple system tauopathy with presenile dementia. *Proc Natl Acad Sci U S A*. 1998;95(13):7737-41.
10. Baker M, Mackenzie IR, Pickering-Brown SM, Gass J, Rademakers R, Lindholm C, et al. Mutations in progranulin cause tau-negative frontotemporal dementia linked to chromosome 17. *Nature*. 2006;442(7105):916-9.
11. Cruts M, Gijssels I, van der Zee J, Engelborghs S, Wils H, Pirici D, et al. Null mutations in progranulin cause ubiquitin-positive frontotemporal dementia linked to chromosome 17q21. *Nature*. 2006;442(7105):920-4.
12. Renton AE, Majounie E, Waite A, Simon-Sanchez J, Rollinson S, Gibbs JR, et al. A hexanucleotide repeat expansion in C9ORF72 is the cause of chromosome 9p21-linked ALS-FTD. *Neuron*. 2011;72(2):257-68.
13. DeJesus-Hernandez M, Mackenzie IR, Boeve BF, Boxer AL, Baker M, Rutherford NJ, et al. Expanded GGGGCC hexanucleotide repeat in noncoding region of C9ORF72 causes chromosome 9p-linked FTD and ALS. *Neuron*. 2011;72(2):245-56.

14. Watts GD, Wymer J, Kovach MJ, Mehta SG, Mumm S, Darvish D, et al. Inclusion body myopathy associated with Paget disease of bone and frontotemporal dementia is caused by mutant valosin-containing protein. *Nat Genet.* 2004;36(4):377-81.
15. Watts GD, Thomasova D, Ramdeen SK, Fulchiero EC, Mehta SG, Drachman DA, et al. Novel VCP mutations in inclusion body myopathy associated with Paget disease of bone and frontotemporal dementia. *Clin Genet.* 2007;72(5):420-6.
16. Borroni B, Bonvicini C, Alberici A, Buratti E, Agosti C, Archetti S, et al. Mutation within TARDBP leads to frontotemporal dementia without motor neuron disease. *Hum Mutat.* 2009;30(11):E974-83.
17. Skibinski G, Parkinson NJ, Brown JM, Chakrabarti L, Lloyd SL, Hummerich H, et al. Mutations in the endosomal ESCRTIII-complex subunit CHMP2B in frontotemporal dementia. *Nat Genet.* 2005;37(8):806-8.
18. Baborie A, Griffiths TD, Jaros E, McKeith IG, Burn DJ, Richardson A, et al. Pathological correlates of frontotemporal lobar degeneration in the elderly. *Acta Neuropathol.* 2011;121(3):365-71.
19. Josephs KA, Hodges JR, Snowden JS, Mackenzie IR, Neumann M, Mann DM, et al. Neuropathological background of phenotypical variability in frontotemporal dementia. *Acta Neuropathol.* 2011;122(2):137-53.
20. Sieben A, Van Langenhove T, Engelborghs S, Martin JJ, Boon P, Cras P, et al. The genetics and neuropathology of frontotemporal lobar degeneration. *Acta Neuropathol.* 2012;124(3):353-72.
21. Gotz J, Halliday G, Nisbet RM. Molecular pathogenesis of the Tauopathies. *Annu Rev Pathol.* 2019;14:239-61.
22. Takada LT. The Genetics of Monogenic Frontotemporal Dementia. *Dement Neuropsychol.* 2015;9(3):219-29.
23. Mackenzie IR. The neuropathology and clinical phenotype of FTD with progranulin mutations. *Acta Neuropathol.* 2007;114(1):49-54.
24. Cairns NJ, Neumann M, Bigio EH, Holm IE, Troost D, Hatanpaa KJ, et al. TDP-43 in familial and sporadic frontotemporal lobar degeneration with ubiquitin inclusions. *Am J Pathol.* 2007;171(1):227-40.
25. Neumann M, Mackenzie IR, Cairns NJ, Boyer PJ, Markesbery WR, Smith CD, et al. TDP-43 in the ubiquitin pathology of frontotemporal dementia with VCP gene mutations. *J Neuropathol Exp Neurol.* 2007;166(2):152-7.
26. Borroni B, Archetti S, Del Bo R, Papetti A, Buratti E, Bonvicini C, et al. TARDBP mutations in frontotemporal lobar degeneration: frequency, clinical features, and disease course. *Rejuvenation Res.* 2010;13(5):509-17.
27. Rohrer JD, Lashley T, Schott JM, Warren JE, Mead S, Isaacs AM, et al. Clinical and neuroanatomical signatures of tissue pathology in frontotemporal lobar degeneration. *Brain.* 2011;134(Pt 9):2565-81.
28. Mackenzie IR, Munoz DG, Kusaka H, Yokota O, Ishihara K, Roeber S, et al. Distinct pathological subtypes of FTL-D-FUS. *Acta Neuropathol.* 2011;121(2):207-18.
29. Mackenzie IR, Neumann M. Molecular neuropathology of frontotemporal dementia: insights into disease mechanisms from postmortem studies. *J Neurochem.* 2016;138 Suppl 1:54-70.
30. Ghosh S, Lippa CF. Clinical Subtypes of Frontotemporal Dementia. *Am J Alzheimers Dis Other Dement.* 2015;30(7):653-61.
31. Lashley T, Rohrer JD, Mead S, Revesz T. Review: an update on clinical, genetic and pathological aspects of frontotemporal lobar degenerations. *Neuropathology and applied neurobiology.* 2015;41(7):858-81.

32. Takahashi K, Yamanaka S. Induction of pluripotent stem cells from mouse embryonic and adult fibroblast cultures by defined factors. *Cell*. 2006;126(4):663-76.
33. Gotz J, Chen F, van Dorpe J, Nitsch RM. Formation of neurofibrillary tangles in P3011 tau transgenic mice induced by A β 42 fibrils. *Science*. 2001;293(5534):1491-5.
34. Lewis J, Dickson DW, Lin WL, Chisholm L, Corral A, Jones G, et al. Enhanced neurofibrillary degeneration in transgenic mice expressing mutant tau and APP. *Science*. 2001;293(5534):1487-91.
35. Hardy J. The discovery of Alzheimer-causing mutations in the APP gene and the formulation of the "amyloid cascade hypothesis". *FEBS J*. 2017;284(7):1040-4.
36. Braak H, Braak E. Neuropathological staging of Alzheimer-related changes. *Acta Neuropathol*. 1991;82(4):239-59.
37. Berg L, McKeel DW, Jr., Miller JP, Storandt M, Rubin EH, Morris JC, et al. Clinicopathologic studies in cognitively healthy aging and Alzheimer's disease: relation of histologic markers to dementia severity, age, sex, and apolipoprotein E genotype. *Arch Neurol*. 1998;55(3):326-35.
38. Guillozet AL, Weintraub S, Mash DC, Mesulam MM. Neurofibrillary tangles, amyloid, and memory in aging and mild cognitive impairment. *Arch Neurol*. 2003;60(5):729-36.
39. Nelson PT, Alafuzoff I, Bigio EH, Bouras C, Braak H, Cairns NJ, et al. Correlation of Alzheimer disease neuropathologic changes with cognitive status: a review of the literature. *J Neuropathol Exp Neurol*. 2012;71(5):362-81.
40. Rapoport M, Dawson HN, Binder LI, Vitek MP, Ferreira A. Tau is essential to beta-amyloid-induced neurotoxicity. *Proc Natl Acad Sci U S A*. 2002;99(9):6364-9.
41. Roberson ED, Scarce-Levie K, Pech J, Yan F, Cheng IH, Wu T, et al. Reducing endogenous tau ameliorates amyloid β -induced deficits in an Alzheimer's disease mouse model. *Science*. 2007;316(5825):750-4.
42. Shipton OA, Leitz JR, Dworzak J, Acton CE, Tunbridge EM, Denk F, et al. Tau protein is required for amyloid β -induced impairment of hippocampal long-term potentiation. *J Neurosci*. 2011;31(5):1558-92.
43. Ke YD, Suchowerska AK, van der Hoven J, De Silva DM, Wu CW, van Eersel J, et al. Lessons from tau-deficient mice. *Int J Alzheimers Dis*. 2012;2012:873270.
44. Goedert M, Spillantini MG, Jakes R, Rutherford D, Crowther RA. Multiple isoforms of human microtubule-associated protein tau: sequences and localization in neurofibrillary tangles of Alzheimer's disease. *Neuron*. 1989;3(4):519-26.
45. Goedert M, Spillantini MG, Potier MC, Ulrich J, Crowther RA. Cloning and sequencing of the cDNA encoding an isoform of microtubule-associated protein tau containing four tandem repeats: differential expression of tau protein mRNAs in human brain. *EMBO J*. 1989;8(2):393-9.
46. Goedert M, Jakes R. Expression of separate isoforms of human tau protein: correlation with the tau pattern in brain and effects on tubulin polymerization. *EMBO J*. 1990;9(13):4225-30.
47. Andreadis A, Broderick JA, Kosik KS. Relative exon affinities and suboptimal splice site signals lead to non-equivalence of two cassette exons. *Nucleic Acids Res*. 1995;23(17):3585-93.
48. Kosik KS, Orecchio LD, Bakalis S, Neve RL. Developmentally regulated expression of specific tau sequences. *Neuron*. 1989;2(4):1389-97.
49. Kar A, Kuo D, He R, Zhou J, Wu JY. Tau alternative splicing and frontotemporal dementia. *Alzheimer Dis Assoc Disord*. 2005;19 Suppl 1:S29-36.
50. Rademakers R, Cruts M, van Broeckhoven C. The role of tau (MAPT) in frontotemporal dementia and related tauopathies. *Hum Mutat*. 2004;24(4):277-95.

51. McCarthy A, Lonergan R, Olszewska DA, O'Dowd S, Cummins G, Magennis B, et al. Closing the tau loop: the missing tau mutation. *Brain*. 2015;138(Pt 10):3100-9.
52. Wszolek ZK, Pfeiffer RF, Bhatt MH, Schelper RL, Cordes M, Snow BJ, et al. Rapidly progressive autosomal dominant parkinsonism and dementia with pallido-ponto-nigral degeneration. *Ann Neurol*. 1992;32(3):312-20.
53. D'Souza I, Poorkaj P, Hong M, Nochlin D, Lee VM, Bird TD, et al. Missense and silent tau gene mutations cause frontotemporal dementia with parkinsonism-chromosome 17 type, by affecting multiple alternative RNA splicing regulatory elements. *Proc Natl Acad Sci U S A*. 1999;96(10):5598-603.
54. Yasuda M, Takamatsu J, D'Souza I, Crowther RA, Kawamata T, Hasegawa M, et al. A novel mutation at position +12 in the intron following exon 10 of the tau gene in familial frontotemporal dementia (FTD-Kumamoto). *Ann Neurol*. 2000;47(4):422-9.
55. Iseki E, Matsumura T, Marui W, Hino H, Odawara T, Sugiyama N, et al. Familial frontotemporal dementia and parkinsonism with a novel N296I mutation in exon 10 of the tau gene and a widespread tau accumulation in the glial cells. *Acta Neuropathol*. 2001;102(3):285-92.
56. Grover A, DeTure M, Yen SH, Hutton M. Effects on splicing and protein function of three mutations in codon N296 of tau in vitro. *Neurosci Lett*. 2002;323(1):33-6.
57. Miyamoto K, Kowalska A, Hasegawa M, Tabira T, Takahashi K, Araki W, et al. Familial frontotemporal dementia and parkinsonism with a novel mutation at an intron 10+11-splice site in the tau gene. *Ann Neurol*. 2001;50(1):117-20.
58. Liu C, Gotz J. Profiling murine tau with 0N, 1N and 2N isoform-specific antibodies in brain and peripheral organs reveals distinct subcellular localization, with the 1N isoform being enriched in the nucleus. *PLoS One*. 2013;8(12):e84849.
59. Mandelkow EM, Stamer K, Vogel R, Thies E, Mandelkow E. Clogging of axons by tau, inhibition of axonal traffic and starvation of synapses. *Neurobiol Aging*. 2003;24(8):1079-85.
60. Deshpande A, Win KM, Busciglio J. Tau isoform expression and regulation in human cortical neurons. *FASEB J*. 2008;22(7):2357-67.
61. Karch CM, Kao AW, Karydas A, Onanuga K, Martinez R, Argouarch A, et al. A Comprehensive Resource for Induced Pluripotent Stem Cells from Patients with Primary Tauopathies. *Stem Cell Reports*. 2019;13(5):939-55.
62. Grover A, Houlden H, Paker M, Adamson J, Lewis J, Prihar G, et al. 5' splice site mutations in tau associated with the inherited dementia FTDP-17 affect a stem-loop structure that regulates alternative splicing of exon 10. *J Biol Chem*. 1999;274(21):15134-43.
63. Patani R, Lewis PA, Trabzuni D, Puddifoot CA, Wyllie DJ, Walker R, et al. Investigating the utility of human embryonic stem cell-derived neurons to model ageing and neurodegenerative disease using whole-genome gene expression and splicing analysis. *J Neurochem*. 2012;122(4):738-51.
64. Handel AE, Chintawar S, Lalic T, Whiteley E, Vowles J, Giustacchini A, et al. Assessing similarity to primary tissue and cortical layer identity in induced pluripotent stem cell-derived cortical neurons through single-cell transcriptomics. *Hum Mol Genet*. 2016;25(5):989-1000.
65. Sposito T, Preza E, Mahoney CJ, Seto-Salvia N, Ryan NS, Morris HR, et al. Developmental regulation of tau splicing is disrupted in stem cell-derived neurons from frontotemporal dementia patients with the 10 + 16 splice-site mutation in MAPT. *Hum Mol Genet*. 2015;24(18):5260-9.
66. Hartfield EM, Yamasaki-Mann M, Ribeiro Fernandes HJ, Vowles J, James WS, Cowley SA, et al. Physiological characterisation of human iPS-derived dopaminergic neurons. *PLoS One*. 2014;9(2):e87388.

67. Iovino M, Agathou S, González-Rueda A, Del Castillo Velasco-Herrera M, Borroni B, Alberici A, et al. Early maturation and distinct tau pathology in induced pluripotent stem cell-derived neurons from patients with MAPT mutations. *Brain*. 2015;138(Pt 11):3345-59.
68. Iovino M, Patani R, Watts C, Chandran S, Spillantini MG. Human stem cell-derived neurons: a system to study human tau function and dysfunction. *PLoS One*. 2010;5(11):e13947.
69. Beevers JE, Lai MC, Collins E, Booth HDE, Zambon F, Parkkinen L, et al. MAPT Genetic Variation and Neuronal Maturity Alter Isoform Expression Affecting Axonal Transport in iPSC-Derived Dopamine Neurons. *Stem Cell Reports*. 2017;9(2):587-99.
70. Paonessa F, Evans LD, Solanki R, Larrieu D, Wray S, Hardy J, et al. Microtubules Deform the Nuclear Membrane and Disrupt Nucleocytoplasmic Transport in Tau-Mediated Frontotemporal Dementia. *Cell Rep*. 2019;26(3):582-93 e5.
71. Sato C, Barthelemy NR, Mawuenyega KG, Patterson BW, Gordon BA, Jockel-Balsarotti J, et al. Tau Kinetics in Neurons and the Human Central Nervous System. *Neuron*. 2018;97(6):1284-98 e7.
72. Espuny-Camacho I, Arranz AM, Fiers M, Snellinx A, Ancón K, Munck S, et al. Hallmarks of Alzheimer's Disease in Stem-Cell-Derived Human Neurons Transplanted into Mouse Brain. *Neuron*. 2017;93(5):1066-81 e8.
73. Choi SH, Kim YH, Hebisch M, Sliwinski C, Lee S, D'Avanzo C, et al. A three-dimensional human neural cell culture model of Alzheimer's disease. *Nature*. 2014;515(7526):274-8.
74. Miguel L, Rovelet-Lecrux A, Feyeux M, Lehoucq T, Nassoy P, Campion D, et al. Detection of all adult Tau isoforms in a 3D culture model of iPSC-derived neurons. *Stem Cell Res*. 2019;40:101541.
75. Lancaster MA, Knoblich JA. Generation of cerebral organoids from human pluripotent stem cells. *Nat Protoc*. 2014;9(10):2329-40.
76. Lancaster MA, Renner M, Martin CA, Wenzel D, Bicknell LS, Hurles ME, et al. Cerebral organoids model human brain development and microcephaly. *Nature*. 2013;501(7467):373-9.
77. Pasca AM, Sloan SA, Clarke LE, Tian Y, Makinson CD, Huber N, et al. Functional cortical neurons and astrocytes from human pluripotent stem cells in 3D culture. *Nat Methods*. 2015;12(7):671-8.
78. Xiang Y, Tanaka Y, Patterson B, Kang YJ, Govindaiah G, Roselaar N, et al. Fusion of Regionally Specified iPSC-Derived Organoids Models Human Brain Development and Interneuron Migration. *Cell Stem Cell*. 2017;21(3):383-98 e7.
79. Krefft O, Jabali A, Jefremova V, Koch P, Ladewig J. Generation of Standardized and Reproducible Forebrain-type Cerebral Organoids from Human Induced Pluripotent Stem Cells. *J Vis Exp*. 2018(131).
80. Vierbuchen T, Ostermeier A, Pang ZP, Kokubu Y, Sudhof TC, Wernig M. Direct conversion of fibroblasts to functional neurons by defined factors. *Nature*. 2010;463(7284):1035-41.
81. Mertens J, Paquola ACM, Ku M, Hatch E, Bohnke L, Ladjevardi S, et al. Directly Reprogrammed Human Neurons Retain Aging-Associated Transcriptomic Signatures and Reveal Age-Related Nucleocytoplasmic Defects. *Cell Stem Cell*. 2015;17(6):705-18.
82. Imamura K, Sahara N, Kanaan NM, Tsukita K, Kondo T, Kutoku Y, et al. Calcium dysregulation contributes to neurodegeneration in FTLD patient iPSC-derived neurons. *Sci Rep*. 2016;6:34904.
83. Verheyen A, Diels A, Reumers J, Van Hoorde K, Van den Wyngaert I, van Outryve d'Ydewalle C, et al. Genetically Engineered iPSC-Derived FTDP-17 MAPT Neurons Display

- Mutation-Specific Neurodegenerative and Neurodevelopmental Phenotypes. *Stem Cell Reports*. 2018;11(2):363-79.
84. Ehrlich M, Hallmann AL, Reinhardt P, Arauzo-Bravo MJ, Korr S, Ropke A, et al. Distinct Neurodegenerative Changes in an Induced Pluripotent Stem Cell Model of Frontotemporal Dementia Linked to Mutant TAU Protein. *Stem Cell Reports*. 2015;5(1):83-96.
 85. Wren MC, Zhao J, Liu CC, Murray ME, Atagi Y, Davis MD, et al. Frontotemporal dementia-associated N279K tau mutant disrupts subcellular vesicle trafficking and induces cellular stress in iPSC-derived neural stem cells. *Mol Neurodegener*. 2015;10:46.
 86. Alonso Adel C, Mederlyova A, Novak M, Grundke-Iqbal I, Iqbal K. Promotion of hyperphosphorylation by frontotemporal dementia tau mutations. *J Biol Chem*. 2004;279(33):34873-81.
 87. Wang JZ, Xia YY, Grundke-Iqbal I, Iqbal K. Abnormal hyperphosphorylation of tau: sites, regulation, and molecular mechanism of neurofibrillary degeneration. *J Alzheimers Dis*. 2013;33 Suppl 1:S123-39.
 88. Hefti MM, Kim S, Bell AJ, Betters RK, Fiock KL, Iida M A, et al. Tau Phosphorylation and Aggregation in the Developing Human Brain. *J Neuropathol Exp Neurol*. 2019;78(10):930-8.
 89. Nakamura M, Shiozawa S, Tsuboi D, Amano M, Watanabe H, Maeda S, et al. Pathological Progression Induced by the Frontotemporal Dementia-Associated R406W Tau Mutation in Patient-Derived iPSCs. *Stem Cell Reports*. 2019;13(4):684-99.
 90. Yu Y, Run X, Liang Z, Li Y, Liu F, Liu Y, et al. Developmental regulation of tau phosphorylation, tau kinases, and tau phosphatases. *J Neurochem*. 2009;108(6):1480-94.
 91. Garcia-Leon JA, Cabrera-Socorro A, Eggermont K, Swijssen A, Terryn J, Fazal R, et al. Generation of a human induced pluripotent stem cell-based model for tauopathies combining three microtubule-associated protein TAU mutations which displays several phenotypes linked to neurodegeneration. *Alzheimers Dement*. 2018;14(10):1261-80.
 92. Demaegd K, Schymkowitz J, Rousseau F. Transcellular Spreading of Tau in Tauopathies. *Chembiochem*. 2018;19(25):2424-32.
 93. Wu JW, Hussaini SA, Bastille IM, Rodriguez GA, Mrejeru A, Rilett K, et al. Neuronal activity enhances tau propagation and tau pathology in vivo. *Nat Neurosci*. 2016;19(8):1085-92.
 94. Evans LD, Wassmer T, Fraser G, Smith J, Perkinton M, Billinton A, et al. Extracellular Monomeric and Aggregated Tau Efficiently Enter Human Neurons through Overlapping but Distinct Pathways. *Cell Rep*. 2018;22(13):3612-24.
 95. Nogales E. Structural insights into microtubule function. *Annu Rev Biochem*. 2000;69:277-302.
 96. Schwarz TL. Mitochondrial trafficking in neurons. *Cold Spring Harb Perspect Biol*. 2013;5(6).
 97. Lin MT, Beal MF. Mitochondrial dysfunction and oxidative stress in neurodegenerative diseases. *Nature*. 2006;443(7113):787-95.
 98. Dixit R, Ross JL, Goldman YE, Holzbaur ELF. Differential Regulation of Dynein and Kinesin Motor Proteins by Tau. *Science*. 2008;319(5866):1086.
 99. Esteras N, Rohrer JD, Hardy J, Wray S, Abramov AY. Mitochondrial hyperpolarization in iPSC-derived neurons from patients of FTDP-17 with 10+16 MAPT mutation leads to oxidative stress and neurodegeneration. *Redox Biol*. 2017;12:410-22.
 100. Biswas MHU, Almeida S, Lopez-Gonzalez R, Mao W, Zhang Z, Karydas A, et al. MMP-9 and MMP-2 Contribute to Neuronal Cell Death in iPSC Models of Frontotemporal Dementia with MAPT Mutations. *Stem Cell Reports*. 2016;7(3):316-24.

101. Kaplan A, Spiller KJ, Towne C, Kanning KC, Choe GT, Geber A, et al. Neuronal matrix metalloproteinase-9 is a determinant of selective neurodegeneration. *Neuron*. 2014;81(2):333-48.
102. Jiang S, Wen N, Li Z, Dube U, Del Aguila J, Budde J, et al. Integrative system biology analyses of CRISPR-edited iPSC-derived neurons and human brains reveal deficiencies of presynaptic signaling in FTL and PSP. *Transl Psychiatry*. 2018;8(1):265.
103. Pooler AM, Phillips EC, Lau DH, Noble W, Hanger DP. Physiological release of endogenous tau is stimulated by neuronal activity. *EMBO Rep*. 2013;14(4):389-94.
104. Kara E, Ling H, Pittman AM, Shaw K, de Silva R, Simone R, et al. The MAPT p.A152T variant is a risk factor associated with tauopathies with atypical clinical and neuropathological features. *Neurobiol Aging*. 2012;33(9):2231 e7- e14.
105. Coppola G, Chinnathambi S, Lee JJ, Dombroski BA, Baker MC, Soto-Ortolaza AI, et al. Evidence for a role of the rare p.A152T variant in MAPT in increasing the risk for FTD-spectrum and Alzheimer's diseases. *Hum Mol Genet*. 2012;21(15):3500-12.
106. Zhang Z, Almeida S, Lu Y, Nishimura AL, Peng L, Sun D, et al. Downregulation of microRNA-9 in iPSC-derived neurons of FTD/ALS patients with TDP-43 mutations. *PLoS One*. 2013;8(10):e76055.
107. Silva MC, Cheng C, Mair W, Almeida S, Fong H, Dias MHU, et al. Human iPSC-Derived Neuronal Model of Tau-A152T Frontotemporal Dementia Reveals Tau-Mediated Mechanisms of Neuronal Vulnerability. *Stem Cell Reports*. 2016;7(3):325-40.
108. Silva MC, Ferguson FM, Cai Q, Donovan KA, Nandi G, Patnaik D, et al. Targeted degradation of aberrant tau in frontotemporal dementia patient-derived neuronal cell models. *Elife*. 2019;8.
109. Baker M, Litvan I, Houlden H, Adame A, Dickson D, Perez-Tur J, et al. Association of an extended haplotype in the tau gene with progressive supranuclear palsy. *Hum Mol Genet*. 1999;8(4):711-5.
110. Conrad C, Andreadis A, Trojanowski JQ, Dickson DW, Kang D, Chen X, et al. Genetic evidence for the involvement of tau in progressive supranuclear palsy. *Ann Neurol*. 1997;41(2):277-81.
111. Caffrey TM, Joachim C, Wade-Martins R. Haplotype-specific expression of the N-terminal exons 2 and 3 at the human MAPT locus. *Neurobiol Aging*. 2008;29(12):1923-9.
112. Trabzuni D, Wray S, Vandrovcova J, Ramasamy A, Walker R, Smith C, et al. MAPT expression and splicing is differentially regulated by brain region: relation to genotype and implication for tauopathies. *Hum Mol Genet*. 2012;21(18):4094-103.
113. Sreedharan J, Blair IP, Tripathi VB, Hu X, Vance C, Rogelj B, et al. TDP-43 mutations in familial and sporadic amyotrophic lateral sclerosis. *Science*. 2008;319(5870):1668-72.
114. Neumann M, Sampathu DM, Kwong LK, Truax AC, Micsenyi MC, Chou TT, et al. Ubiquitinated TDP-43 in frontotemporal lobar degeneration and amyotrophic lateral sclerosis. *Science*. 2006;314(5796):130-3.
115. Arai T, Hasegawa M, Akiyama H, Ikeda K, Nonaka T, Mori H, et al. TDP-43 is a component of ubiquitin-positive tau-negative inclusions in frontotemporal lobar degeneration and amyotrophic lateral sclerosis. *Biochem Biophys Res Commun*. 2006;351(3):602-11.
116. Neumann M, Kwong LK, Lee EB, Kremmer E, Flatley A, Xu Y, et al. Phosphorylation of S409/410 of TDP-43 is a consistent feature in all sporadic and familial forms of TDP-43 proteinopathies. *Acta Neuropathol*. 2009;117(2):137-49.
117. Nonaka T, Kametani F, Arai T, Akiyama H, Hasegawa M. Truncation and pathogenic mutations facilitate the formation of intracellular aggregates of TDP-43. *Hum Mol Genet*. 2009;18(18):3353-64.

118. Floris G, Borghero G, Cannas A, Di Stefano F, Murru MR, Corongiu D, et al. Clinical phenotypes and radiological findings in frontotemporal dementia related to TARDBP mutations. *J Neurol*. 2015;262(2):375-84.
119. Kovacs GG, Murrell JR, Horvath S, Haraszti L, Majtenyi K, Molnar MJ, et al. TARDBP variation associated with frontotemporal dementia, supranuclear gaze palsy, and chorea. *Mov Disord*. 2009;24(12):1843-7.
120. Amador-Ortiz C, Lin WL, Ahmed Z, Personett D, Davies P, Duara R, et al. TDP-43 immunoreactivity in hippocampal sclerosis and Alzheimer's disease. *Ann Neurol*. 2007;61(5):435-45.
121. Dardis A, Zampieri S, Canterini S, Newell KL, Stuani C, Murrell JR, et al. Altered localization and functionality of TAR DNA Binding Protein 43 (TDP-43) in niemann-pick disease type C. *Acta Neuropathol Commun*. 2016;4(1):52.
122. Jayakumar AR, Tong XY, Shamaladevi N, Barcelona S, Gaidosh G, Agarwal A, et al. Defective synthesis and release of astrocytic thrombospondin-1 mediates the neuronal TDP-43 proteinopathy, resulting in defects in neuronal integrity associated with chronic traumatic encephalopathy: in vitro studies. *J Neurochem*. 2017;140(4):645-61.
123. McAleese KE, Walker L, Erskine D, Thomas AJ, McKeith IG, Attems J. TDP-43 pathology in Alzheimer's disease, dementia with Lewy bodies and ageing. *Brain Pathol*. 2017;27(4):472-9.
124. Wright DK, Liu S, van der Poel C, McDonald SJ, Brady RD, Taylor L, et al. Traumatic Brain Injury Results in Cellular, Structural and Functional Changes Resembling Motor Neuron Disease. *Cereb Cortex*. 2017;27(9):2503-15.
125. Buratti E. TDP-43 post-translational modifications in health and disease. *Expert Opin Ther Targets*. 2018;22(3):279-93.
126. Zhang YJ, Gendron TF, Xu YF, Ko LW, Yen SH, Petrucelli L. Phosphorylation regulates proteasomal-mediated degradation and solubility of TAR DNA binding protein-43 C-terminal fragments. *Mol Neurodegener*. 2010;5:33.
127. Cohen TJ, Hwang AW, Restrepo CR, Yuan CX, Trojanowski JQ, Lee VM. An acetylation switch controls TDP-43 function and aggregation propensity. *Nat Commun*. 2015;6:5845.
128. Tanji K, Zhang HX, Mori F, Kakita A, Takahashi H, Wakabayashi K. p62/sequestosome 1 binds to TDP-43 in brains with frontotemporal lobar degeneration with TDP-43 inclusions. *J Neurosci Res*. 2012;90(10):2034-42.
129. Ayala YM, Zago P, L'Ambrogio A, Xu YF, Petrucelli L, Buratti E, et al. Structural determinants of the cellular localization and shuttling of TDP-43. *J Cell Sci*. 2008;121(Pt 22):3778-85.
130. Gijssels I, Van Broeckhoven C, Cruts M. Granulin mutations associated with frontotemporal lobar degeneration and related disorders: an update. *Hum Mutat*. 2008;29(12):1373-86.
131. Yu CE, Bird TD, Bekris LM, Montine TJ, Leverenz JB, Steinbart E, et al. The spectrum of mutations in progranulin: a collaborative study screening 545 cases of neurodegeneration. *Arch Neurol*. 2010;67(2):161-70.
132. Gass J, Cannon A, Mackenzie IR, Boeve B, Baker M, Adamson J, et al. Mutations in progranulin are a major cause of ubiquitin-positive frontotemporal lobar degeneration. *Hum Mol Genet*. 2006;15(20):2988-3001.
133. Rademakers R, Baker M, Gass J, Adamson J, Huey ED, Momeni P, et al. Phenotypic variability associated with progranulin haploinsufficiency in patients with the common 1477C->T (Arg493X) mutation: an international initiative. *Lancet Neurol*. 2007;6(10):857-68.

134. Arrant AE, Nicholson AM, Zhou X, Rademakers R, Roberson ED. Partial Tmem106b reduction does not correct abnormalities due to progranulin haploinsufficiency. *Mol Neurodegener.* 2018;13(1):32.
135. Kessenbrock K, Frohlich L, Sixt M, Lammermann T, Pfister H, Bateman A, et al. Proteinase 3 and neutrophil elastase enhance inflammation in mice by inactivating antiinflammatory progranulin. *J Clin Invest.* 2008;118(7):2438-47.
136. Zhu J, Nathan C, Jin W, Sim D, Ashcroft GS, Wahl SM, et al. Conversion of proepithelin to epithelins: roles of SLPI and elastase in host defense and wound repair. *Cell.* 2002;111(6):867-78.
137. Suh HS, Choi N, Tarassishin L, Lee SC. Regulation of progranulin expression in human microglia and proteolysis of progranulin by matrix metalloproteinase-12 (MMP-12). *PLoS One.* 2012;7(4):e35115.
138. Holler CJ, Taylor G, Deng Q, Kukar T. Intracellular Proteolysis of Progranulin Generates Stable, Lysosomal Granulins that Are Haploinsufficient in Patients with Frontotemporal Dementia Caused by GRN Mutations. *eNeuro.* 2017;4(4).
139. Gao X, Joselin AP, Wang L, Kar A, Ray P, Bateman A, et al. Progranulin promotes neurite outgrowth and neuronal differentiation by regulating CSK-3 beta. *Protein Cell.* 2010;1(6):552-62.
140. Yin F, Banerjee R, Thomas B, Zhou P, Qian L, Jia T, et al. Exaggerated inflammation, impaired host defense, and neuropathology in progranulin-deficient mice. *J Exp Med.* 2010;207(1):117-28.
141. Uesaka N, Abe M, Konno K, Yamazaki M, Sakoori K, Watanabe T, et al. Retrograde Signaling from Progranulin to Sort1 Counteracts Synapse Elimination in the Developing Cerebellum. *Neuron.* 2018;97(4):796-805 e5.
142. Smith KR, Damiano J, Franceschetti S, Carpenter S, Canafoglia L, Morbin M, et al. Strikingly different clinicopathological phenotypes determined by progranulin-mutation dosage. *Am J Hum Genet.* 2012;90(6):1102-7.
143. Canafoglia L, Morbin M, Scuderi V, Pareyson D, D'Incerti L, Fugnanesi V, et al. Recurrent generalized seizures, visual loss, and palinopsia as phenotypic features of neuronal ceroid lipofuscinosis due to progranulin gene mutation. *Epilepsia.* 2014;55(6):e56-9.
144. Almeida MR, Macario MC, Ramos L, Baldeiras I, Ribeiro MH, Santana I. Portuguese family with the co-occurrence of frontotemporal lobar degeneration and neuronal ceroid lipofuscinosis phenotypes due to progranulin gene mutation. *Neurobiol Aging.* 2016;41:200 e1- e5.
145. Gotzl JK, Mori K, Damme M, Fellerer K, Tahirovic S, Kleinberger G, et al. Common pathobiochemical hallmarks of progranulin-associated frontotemporal lobar degeneration and neuronal ceroid lipofuscinosis. *Acta Neuropathol.* 2014;127(6):845-60.
146. Ward ME, Chen R, Huang HY, Ludwig C, Telpoukhovskaia M, Taubes A, et al. Individuals with progranulin haploinsufficiency exhibit features of neuronal ceroid lipofuscinosis. *Sci Transl Med.* 2017;9(385).
147. Ahmed Z, Sheng H, Xu YF, Lin WL, Innes AE, Gass J, et al. Accelerated lipofuscinosis and ubiquitination in granulin knockout mice suggest a role for progranulin in successful aging. *Am J Pathol.* 2010;177(1):311-24.
148. Wils H, Kleinberger G, Pereson S, Janssens J, Capell A, Van Dam D, et al. Cellular ageing, increased mortality and FTLTDP-associated neuropathology in progranulin knockout mice. *J Pathol.* 2012;228(1):67-76.
149. Jian J, Tian QY, Hettinghouse A, Zhao S, Liu H, Wei J, et al. Progranulin Recruits HSP70 to beta-Glucocerebrosidase and Is Therapeutic Against Gaucher Disease. *EBioMedicine.* 2016;13:212-24.

150. Beel S, Moisse M, Damme M, De Muynck L, Robberecht W, Van Den Bosch L, et al. Progranulin functions as a cathepsin D chaperone to stimulate axonal outgrowth in vivo. *Hum Mol Genet.* 2017;26(15):2850-63.
151. Valdez C, Wong YC, Schwake M, Bu G, Wszolek ZK, Krainc D. Progranulin-mediated deficiency of cathepsin D results in FTD and NCL-like phenotypes in neurons derived from FTD patients. *Hum Mol Genet.* 2017;26(24):4861-72.
152. Zhou X, Paushter DH, Feng T, Sun L, Reinheckel T, Hu F. Lysosomal processing of progranulin. *Mol Neurodegener.* 2017;12(1):62.
153. Butler VJ, Cortopassi WA, Argouarch AR, Ivry SL, Craik CS, Jacobson MP, et al. Progranulin Stimulates the In Vitro Maturation of Pro-Cathepsin D at Acidic pH. *J Mol Biol.* 2019;431(5):1038-47.
154. Ketscher A, Ketterer S, Dollwet-Mack S, Reif U, Reinheckel T. Neuroectoderm-specific deletion of cathepsin D in mice models human inherited neuronal ceroid lipofuscinosis type 10. *Biochimie.* 2016;122:219-26.
155. Ketterer S, Gomez-Auli A, Hillebrand LE, Petrera A, Ketscher A, Reinheckel T. Inherited diseases caused by mutations in cathepsin protease gene. *FEBS J.* 2017;284(10):1437-54.
156. Almeida S, Zhang Z, Coppola G, Mao W, Futai K, Karydas A, et al. Induced pluripotent stem cell models of progranulin-deficient frontotemporal dementia uncover specific reversible neuronal defects. *Cell Rep.* 2012;2(4):189-98.
157. Zhang YJ, Xu YF, Dickey CA, Buratti E, Barallic F, Bailey R, et al. Progranulin mediates caspase-dependent cleavage of TAR DNA binding protein-43. *J Neurosci.* 2007;27(39):10530-4.
158. Lee WC, Almeida S, Prudencio M, Caulfield TR, Zhang YJ, Tay WM, et al. Targeted manipulation of the sortilin-progranulin axis rescues progranulin haploinsufficiency. *Hum Mol Genet.* 2014;23(6):1467-78.
159. Gascon E, Lynch K, Ruan H, Almeida S, Verheyden JM, Seeley WW, et al. Alterations in microRNA-124 and *APP* receptors contribute to social behavioral deficits in frontotemporal dementia. *Nat Med.* 2014;20(12):1444-51.
160. Almeida S, Gao F, Coppola G, Gao FB. Suberoylanilide hydroxamic acid increases progranulin production in iPSC derived cortical neurons of frontotemporal dementia patients. *Neurobiol Aging.* 2016;42:35-40.
161. Lee CW, Stankowski JN, Chew J, Cook CN, Lam YW, Almeida S, et al. The lysosomal protein cathepsin D is a progranulin protease. *Mol Neurodegener.* 2017;12(1):55.
162. Hu F, Padukkavidana T, Vaegter CB, Brady OA, Zheng Y, Mackenzie IR, et al. Sortilin-mediated endocytosis determines levels of the frontotemporal dementia protein, progranulin. *Neuron.* 2010;68(4):654-67.
163. Holler CJ, Taylor G, McEachin ZT, Deng Q, Watkins WJ, Hudson K, et al. Trehalose upregulates progranulin expression in human and mouse models of GRN haploinsufficiency: a novel therapeutic lead to treat frontotemporal dementia. *Mol Neurodegener.* 2016;11(1):46.
164. Mason AR, Elia LP, Finkbeiner S. The Receptor-interacting Serine/Threonine Protein Kinase 1 (RIPK1) Regulates Progranulin Levels. *J Biol Chem.* 2017;292(8):3262-72.
165. Elia LP, Mason AR, Alijagic A, Finkbeiner S. Genetic Regulation of Neuronal Progranulin Reveals a Critical Role for the Autophagy-Lysosome Pathway. *J Neurosci.* 2019;39(17):3332-44.
166. Tian R, Gachechiladze MA, Ludwig CH, Laurie MT, Hong JY, Nathaniel D, et al. CRISPR Interference-Based Platform for Multimodal Genetic Screens in Human iPSC-Derived Neurons. *Neuron.* 2019;104(2):239-55 e12.

167. Visvanathan J, Lee S, Lee B, Lee JW, Lee SK. The microRNA miR-124 antagonizes the anti-neural REST/SCP1 pathway during embryonic CNS development. *Genes Dev.* 2007;21(7):744-9.
168. Gao FB. Context-dependent functions of specific microRNAs in neuronal development. *Neural Dev.* 2010;5:25.
169. Ho VM, Dallalzadeh LO, Karathanasis N, Keles MF, Vangala S, Grogan T, et al. GluA2 mRNA distribution and regulation by miR-124 in hippocampal neurons. *Mol Cell Neurosci.* 2014;61:1-12.
170. Hou Q, Ruan H, Gilbert J, Wang G, Ma Q, Yao WD, et al. MicroRNA miR124 is required for the expression of homeostatic synaptic plasticity. *Nat Commun.* 2015;6:10045.
171. Raitano S, Ordovas L, De Muynck L, Guo W, Espuny-Camacho I, Geraerts M, et al. Restoration of progranulin expression rescues cortical neuron generation in an induced pluripotent stem cell model of frontotemporal dementia. *Stem Cell Reports.* 2015;4(1):16-24.
172. Chang MC, Srinivasan K, Friedman BA, Suto E, Modrusan Z, Lee WP, et al. Progranulin deficiency causes impairment of autophagy and TDP-43 accumulation. *J Exp Med.* 2017;214(9):2611-28.
173. Gotzl JK, Brendel M, Werner G, Parhizkar S, Sebastian Monasor L, Kleinberger G, et al. Opposite microglial activation stages upon loss of PCRN1 or TREM2 result in reduced cerebral glucose metabolism. *EMBO Mol Med.* 2019;11(6).
174. Evers BM, Rodriguez-Navas C, Tesla RJ, Prange-Kiel J, Wasser CR, Yoo KS, et al. Lipidomic and Transcriptomic Basis of Lysosomal Dysfunction in Progranulin Deficiency. *Cell Rep.* 2017;20(11):2565-74.
175. Marschallinger J, Iram T, Zardeneta M, Lee SE, Lehallier B, Haney MS, et al. Lipid-droplet-accumulating microglia represent a dysfunctional and proinflammatory state in the aging brain. *Nat Neurosci.* 2020.
176. Hasselmann J, Blurton-Jones M. Human iPSC-derived microglia: A growing toolset to study the brain's innate immune cells. *Glia.* 2020.
177. Marogianni C, Rikos D, Proietta A, Dadouli K, Ntellas P, Tsitsi P, et al. The role of C9orf72 in neurodegenerative disorders: a systematic review, an updated meta-analysis, and the creation of an online database. *Neurobiol Aging.* 2019;84:238.e25-.e34.
178. Rutherford NJ, Heckman MG, Dejesus-Hernandez M, Baker MC, Soto-Ortolaza AI, Rayaprolu S, et al. Length of normal alleles of C9ORF72 GGGGCC repeat do not influence disease phenotype. *Neurobiol Aging.* 2012;33(12):2950 e5-7.
179. van der Zee J, Gijssels I, Dillen L, Van Langenhove T, Theuns J, Engelborghs S, et al. A pan-European study of the C9orf72 repeat associated with FTLD: geographic prevalence, genomic instability, and intermediate repeats. *Hum Mutat.* 2013;34(2):363-73.
180. Levine TP, Daniels RD, Gatta AT, Wong LH, Hayes MJ. The product of C9orf72, a gene strongly implicated in neurodegeneration, is structurally related to DENN Rab-GEFs. *Bioinformatics.* 2013;29(4):499-503.
181. Farg MA, Sundaramoorthy V, Sultana JM, Yang S, Atkinson RA, Levina V, et al. C9ORF72, implicated in amyotrophic lateral sclerosis and frontotemporal dementia, regulates endosomal trafficking. *Hum Mol Genet.* 2014;23(13):3579-95.
182. Webster CP, Smith EF, Bauer CS, Moller A, Hautbergue GM, Ferraiuolo L, et al. The C9orf72 protein interacts with Rab1a and the ULK1 complex to regulate initiation of autophagy. *EMBO J.* 2016;35(15):1656-76.
183. Sellier C, Campanari ML, Julie Corbier C, Gaucherot A, Kolb-Cheynel I, Oulad-Abdelghani M, et al. Loss of C9ORF72 impairs autophagy and synergizes with polyQ Ataxin-2 to induce motor neuron dysfunction and cell death. *EMBO J.* 2016;35(12):1276-97.

184. O'Rourke JG, Bogdanik L, Yanez A, Lall D, Wolf AJ, Muhammad AK, et al. C9orf72 is required for proper macrophage and microglial function in mice. *Science*. 2016;351(6279):1324-9.
185. Sullivan PM, Zhou X, Robins AM, Paushter DH, Kim D, Smolka MB, et al. The ALS/FTLD associated protein C9orf72 associates with SMCR8 and WDR41 to regulate the autophagy-lysosome pathway. *Acta Neuropathol Commun*. 2016;4(1):51.
186. Yang M, Liang C, Swaminathan K, Herrlinger S, Lai F, Shiekhattar R, et al. A C9ORF72/SMCR8-containing complex regulates ULK1 and plays a dual role in autophagy. *Sci Adv*. 2016;2(9):e1601167.
187. Ugolino J, Ji YJ, Conchina K, Chu J, Nirujogi RS, Pandey A, et al. Loss of C9orf72 Enhances Autophagic Activity via Deregulated mTOR and TFEB Signaling. *PLoS Genet*. 2016;12(11):e1006443.
188. Amick J, Roczniak-Ferguson A, Ferguson SM. C9orf72 binds SMCR8, localizes to lysosomes, and regulates mTORC1 signaling. *Mol Biol Cell*. 2016;27(20):3040-51.
189. Aoki Y, Manzano R, Lee Y, Dafinca R, Aoki M, Douglas AGL, et al. C9orf72 and RAB7L1 regulate vesicle trafficking in amyotrophic lateral sclerosis and frontotemporal dementia. *Brain*. 2017;140(4):887-97.
190. Gijssels I, Van Langenhove T, van der Zee J, Sleegers K, Philtjens S, Kleinberger G, et al. A C9orf72 promoter repeat expansion in a Flanders-Belgian cohort with disorders of the frontotemporal lobar degeneration-amyotrophic lateral sclerosis spectrum: a gene identification study. *Lancet Neurol*. 2012;11(1):54-65.
191. van Blitterswijk M, Gendron TF, Baker MV, DeJesus-Hernandez M, Finch NA, Brown PH, et al. Novel clinical associations with specific C9ORF72 transcripts in patients with repeat expansions in C9ORF72. *Acta Neuropathol*. 2015;130(6):863-76.
192. Lee YB, Chen HJ, Peres JN, Gomez-Deza J, Attig J, Stalekar M, et al. Hexanucleotide repeats in ALS/FTD form length-dependent RNA foci, sequester RNA binding proteins, and are neurotoxic. *Cell Rep*. 2013;5(5):1178-86.
193. Ash PE, Bieniek KF, Gendron TF, Caulfield T, Lin WL, DeJesus-Hernandez M, et al. Unconventional translation of C9ORF72 GGGGCC expansion generates insoluble polypeptides specific to c9FTD/ALS. *Neuron*. 2013;77(4):639-46.
194. Mori K, Weng SM, Arzberger T, May S, Rentzsch K, Kremmer E, et al. The C9orf72 GGGGCC repeat is translated into aggregating dipeptide-repeat proteins in FTD/ALS. *Science*. 2013;339(6125):1355-3.
195. Gendron TF, Bieniek KF, Zhang YJ, Jansen-West K, Ash PE, Caulfield T, et al. Antisense transcripts of the expanded C9ORF72 hexanucleotide repeat form nuclear RNA foci and undergo repeat-associated non-ATG translation in c9FTD/ALS. *Acta Neuropathol*. 2013;126(6):829-44.
196. Nordin A, Akimoto C, Wuolikainen A, Alstermark H, Jonsson P, Birve A, et al. Extensive size variability of the GGGGCC expansion in C9orf72 in both neuronal and non-neuronal tissues in 18 patients with ALS or FTD. *Hum Mol Genet*. 2015;24(11):3133-42.
197. Almeida S, Gascon E, Tran H, Chou HJ, Gendron TF, Degroot S, et al. Modeling key pathological features of frontotemporal dementia with C9ORF72 repeat expansion in iPSC-derived human neurons. *Acta Neuropathol*. 2013;126(3):385-99.
198. Sareen D, O'Rourke JG, Meera P, Muhammad AK, Grant S, Simpkinson M, et al. Targeting RNA foci in iPSC-derived motor neurons from ALS patients with a C9ORF72 repeat expansion. *Sci Transl Med*. 2013;5(208):208ra149.
199. Dafinca R, Scaber J, Ababneh N, Lalic T, Weir G, Christian H, et al. C9orf72 Hexanucleotide Expansions Are Associated with Altered Endoplasmic Reticulum Calcium Homeostasis and Stress Granule Formation in Induced Pluripotent Stem Cell-Derived

- Neurons from Patients with Amyotrophic Lateral Sclerosis and Frontotemporal Dementia. *Stem Cells*. 2016;34(8):2063-78.
200. Esanov R, Belle KC, van Blitterswijk M, Belzil VV, Rademakers R, Dickson DW, et al. C9orf72 promoter hypermethylation is reduced while hydroxymethylation is acquired during reprogramming of ALS patient cells. *Exp Neurol*. 2016;277:171-7.
201. Bardelli D, Sassone F, Colombrita C, Volpe C, Gumina V, Peverelli S, et al. Reprogramming fibroblasts and peripheral blood cells from a C9ORF72 patient: A proof-of-principle study. *Journal of Cellular and Molecular Medicine*. 2020;24(7):4051-60.
202. Simone R, Balendra R, Moens TG, Preza E, Wilson KM, Heslegrave A, et al. G-quadruplex-binding small molecules ameliorate C9orf72 FTD/ALS pathology in vitro and in vivo. *EMBO molecular medicine*. 2018;10(1):22-31.
203. Yuva-Aydemir Y, Almeida S, Krishnan G, Gendron TF, Gao F-B. Transcription elongation factor AFF2/FMR2 regulates expression of expanded GGGGCC repeat-containing C9ORF72 allele in ALS/FTD. *Nature Communications*. 2019;10(1):5466.
204. Donnelly CJ, Zhang PW, Pham JT, Haeusler AR, Mistry NA, Vidensky S, et al. RNA toxicity from the ALS/FTD C9ORF72 expansion is mitigated by antisense intervention. *Neuron*. 2013;80(2):415-28.
205. Lopez-Gonzalez R, Lu Y, Gendron Tania F, Karimdas A, Tran H, Yang D, et al. Poly(GR) in C9ORF72-Related ALS/FTD Compromises Mitochondrial Function and Increases Oxidative Stress and DNA Damage in iPSC-Derived Motor Neurons. *Neuron*. 2016;92(2):383-91.
206. Selvaraj BT, Livesey MR, Zhao C, Gregory JM, James OT, Cleary EM, et al. C9ORF72 repeat expansion causes vulnerability of motor neurons to Ca(2+)-permeable AMPA receptor-mediated excitotoxicity. *Nat Commun*. 2018;9(1):347.
207. Ababneh NA, Scaber J, Flynn R, Douglas A, Barbagallo P, Candalija A, et al. Correction of amyotrophic lateral sclerosis related phenotypes in induced pluripotent stem cell-derived motor neurons carrying a hexanucleotide expansion mutation in C9orf72 by CRISPR/Cas9 genome editing using homology-directed repair. *Human Molecular Genetics*. 2020;29(13):2200-17.
208. Zhao C, Devlin AC, Chohan AK, Selvaraj BT, Stavrou M, Burr K, et al. Mutant C9orf72 human iPSC-derived astrocytes cause non-cell autonomous motor neuron pathophysiology. *Glia*. 2020;62(5):1046-64.
209. Zhang K, Donnelly CJ, Haeusler AR, Grima JC, Machamer JB, Steinwald P, et al. The C9orf72 repeat expansion disrupts nucleocytoplasmic transport. *Nature*. 2015;525(7567):56-61.
210. Jiang H, Mankodi A, Swanson MS, Moxley RT, Thornton CA. Myotonic dystrophy type 1 is associated with nuclear foci of mutant RNA, sequestration of muscleblind proteins and deregulated alternative splicing in neurons. *Human Molecular Genetics*. 2004;13(24):3079-88.
211. Westergard T, Jensen BK, Wen X, Cai J, Kropf E, Iacovitti L, et al. Cell-to-Cell Transmission of Dipeptide Repeat Proteins Linked to C9orf72-ALS/FTD. *Cell Rep*. 2016;17(3):645-52.
212. Shi Y, Lin S, Staats KA, Li Y, Chang WH, Hung ST, et al. Haploinsufficiency leads to neurodegeneration in C9ORF72 ALS/FTD human induced motor neurons. *Nat Med*. 2018;24(3):313-25.
213. Sivadasan R, Hornburg D, Drepper C, Frank N, Jablonka S, Hansel A, et al. C9ORF72 interaction with cofilin modulates actin dynamics in motor neurons. *Nat Neurosci*. 2016;19(12):1610-8.

214. Xi Z, Zinman L, Moreno D, Schymick J, Liang Y, Sato C, et al. Hypermethylation of the CpG island near the G4C2 repeat in ALS with a C9orf72 expansion. *Am J Hum Genet.* 2013;92(6):981-9.
215. Xi Z, Rainero I, Rubino E, Pinessi L, Bruni AC, Maletta RG, et al. Hypermethylation of the CpG-island near the C9orf72 G(4)C(2)-repeat expansion in FTLD patients. *Hum Mol Genet.* 2014;23(21):5630-7.
216. Belzil VV, Bauer PO, Gendron TF, Murray ME, Dickson D, Petrucelli L. Characterization of DNA hypermethylation in the cerebellum of c9FTD/ALS patients. *Brain research.* 2014;1584:15-21.
217. Xi Z, Zhang M, Bruni AC, Maletta RG, Colao R, Fratta P, et al. The C9orf72 repeat expansion itself is methylated in ALS and FTLD patients. *Acta Neuropathol.* 2015;129(5):715-27.
218. Russ J, Liu EY, Wu K, Neal D, Suh E, Irwin DJ, et al. Hypermethylation of repeat expanded C9orf72 is a clinical and molecular disease modifier. *Acta Neuropathol.* 2015;129(1):39-52.
219. Cohen-Hadad Y, Altarescu G, Eldar-Geva T, Levi-Lavad J, Zhang M, Rogaeva E, et al. Marked Differences in C9orf72 Methylation Status and Isoform Expression between C9/ALS Human Embryonic and Induced Pluripotent Stem Cells. *Stem Cell Reports.* 2016;7(5):927-40.
220. Ratti A, Gumina V, Lenzi P, Bossolasco P, Filceri F, Volpe C, et al. Chronic stress induces formation of stress granules and pathological TDP-43 aggregates in human ALS fibroblasts and iPSC-motoneurons. *Neurobiol Dis.* 2020:105051.
221. Mackenzie IR, Frick P, Neumann M. The neuropathology associated with repeat expansions in the C9ORF72 gene. *Acta Neuropathol.* 2014;127(3):347-57.
222. Freibaum BD, Lu Y, Lopez-Gonzalez R, Kim NC, Almeida S, Lee KH, et al. GGGGCC repeat expansion in C9orf72 compromises nucleocytoplasmic transport. *Nature.* 2015;525(7567):129-33.
223. Jovicic A, Mertens J, Boeynens S, Bogaert E, Chai N, Yamada SB, et al. Modifiers of C9orf72 dipeptide repeat toxicity connect nucleocytoplasmic transport defects to FTD/ALS. *Nat Neurosci.* 2015;18(9):1226-9.
224. Cheng W, Wang S, Zhang Z, Morgens DW, Hayes LR, Lee S, et al. CRISPR-Cas9 Screens Identify the RNA Helicase DDX3X as a Repressor of C9ORF72 (GGGGCC)_n Repeat-Associated Non-AUG Translation. *Neuron.* 2019;104(5):885-98 e8.
225. Moore S, Alsop JJ, Lorenzini I, Starr A, Rabichow BE, Mendez E, et al. ADAR2 mislocalization and widespread RNA editing aberrations in C9orf72-mediated ALS/FTD. *Acta Neuropathol.* 2019;138(1):49-65.
226. Andrade NS, Ramic M, Esanov R, Liu W, Rybin MJ, Gaidosh G, et al. Dipeptide repeat proteins inhibit homology-directed DNA double strand break repair in C9ORF72 ALS/FTD. *Molecular Neurodegeneration.* 2020;15(1):13.
227. Abo-Rady M, Kalmbach N, Pal A, Schludi C, Janosch A, Richter T, et al. Knocking out C9ORF72 Exacerbates Axonal Trafficking Defects Associated with Hexanucleotide Repeat Expansion and Reduces Levels of Heat Shock Proteins. *Stem Cell Reports.* 2020;14(3):390-405.
228. Coyne AN, Lorenzini I, Chou CC, Torvund M, Rogers RS, Starr A, et al. Post-transcriptional Inhibition of Hsc70-4/HSPA8 Expression Leads to Synaptic Vesicle Cycling Defects in Multiple Models of ALS. *Cell Rep.* 2017;21(1):110-25.
229. Porterfield V, Khan SS, Foff EP, Koseoglu MM, Blanco IK, Jayaraman S, et al. A three-dimensional dementia model reveals spontaneous cell cycle re-entry and a senescence-associated secretory phenotype. *Neurobiology of Aging.* 2020;90:125-34.

230. Williams KL, Fifita JA, Vucic S, Durnall JC, Kiernan MC, Blair IP, et al. Pathophysiological insights into ALS with C9ORF72 expansions. *J Neurol Neurosurg Psychiatry*. 2013;84(8):931-5.
231. Devlin AC, Burr K, Borooah S, Foster JD, Cleary EM, Geti I, et al. Human iPSC-derived motoneurons harbouring TARDBP or C9ORF72 ALS mutations are dysfunctional despite maintaining viability. *Nat Commun*. 2015;6:5999.
232. Wainger BJ, Kiskinis E, Mellin C, Wiskow O, Han SS, Sandoe J, et al. Intrinsic membrane hyperexcitability of amyotrophic lateral sclerosis patient-derived motor neurons. *Cell Rep*. 2014;7(1):1-11.
233. Meyer K, Ferraiuolo L, Miranda CJ, Likhite S, McElroy S, Rensch S, et al. Direct conversion of patient fibroblasts demonstrates non-cell autonomous toxicity of astrocytes to motor neurons in familial and sporadic ALS. *Proc Natl Acad Sci U S A*. 2014;111(2):829-32.
234. Madill M, McDonagh K, Ma J, Vajda A, McLoughlin P, O'Brien T, et al. Amyotrophic lateral sclerosis patient iPSC-derived astrocytes impair autophagy via non-cell autonomous mechanisms. *Molecular Brain*. 2017;10(1):22.
235. Birger A, Ben-Dor I, Ottolenghi M, Turetsky T, Gil Y, Sweetat S, et al. Human iPSC-derived astrocytes from ALS patients with mutated C9ORF72 show increased oxidative stress and neurotoxicity. *EBioMedicine*. 2019;50:274-89.
236. Varcianna A, Myszczyńska MA, Castelli LM, O'Neill B, Kim Y, Talbot J, et al. Micro-RNAs secreted through astrocyte-derived extracellular vesicles cause neuronal network degeneration in C9orf72 ALS. *EBioMedicine*. 2019;40:626-35.
237. Ferraiuolo L, Meyer K, Sherwood TW, Vick J, Likhite S, Frakes A, et al. Oligodendrocytes contribute to motor neuron death in ALS via SOD1-dependent mechanism. *Proceedings of the National Academy of Sciences*. 2016;113(42):E6496-E505.
238. Imamura K, Izumi Y, Watanabe A, Tsukita K, Woltjen K, Yamamoto T, et al. The Src/c-Abl pathway is a potential therapeutic target in amyotrophic lateral sclerosis. *Sci Transl Med*. 2017;9(391).
239. Bilican B, Serio A, Barmada SJ, Nishimura AL, Sullivan GJ, Carrasco M, et al. Mutant induced pluripotent stem cell lines recapitulate aspects of TDP-43 proteinopathies and reveal cell-specific vulnerability. *Proc Natl Acad Sci U S A*. 2012;109(15):5803-8.
240. Serio A, Bilican B, Barmada SJ, Ando DM, Zhao C, Siller R, et al. Astrocyte pathology and the absence of non-cell autonomy in an induced pluripotent stem cell model of TDP-43 proteinopathy. *Proc Natl Acad Sci U S A*. 2013;110(12):4697-702.
241. Nagai M, Reed DB, Najata T, Chalazonitis A, Jessell TM, Wichterle H, et al. Astrocytes expressing ALS-linked mutated SOD1 release factors selectively toxic to motor neurons. *Nat Neurosci*. 2007;10(5):615-22.
242. Bossolasco P, Sassone F, Gumina V, Peverelli S, Garzo M, Silani V. Motor neuron differentiation of iPSCs obtained from peripheral blood of a mutant TARDBP ALS patient. *Stem Cell Res*. 2018;30:61-8.
243. Egawa N, Kitaoka S, Tsukita K, Naitoh M, Takahashi K, Yamamoto T, et al. Drug screening for ALS using patient-specific induced pluripotent stem cells. *Sci Transl Med*. 2012;4(145):145ra04.
244. Kreiter N, Pal A, Lojewski X, Corcia P, Naujock M, Reinhardt P, et al. Age-dependent neurodegeneration and organelle transport deficiencies in mutant TDP43 patient-derived neurons are independent of TDP43 aggregation. *Neurobiol Dis*. 2018;115:167-81.
245. Burkhardt MF, Martinez FJ, Wright S, Ramos C, Volfson D, Mason M, et al. A cellular model for sporadic ALS using patient-derived induced pluripotent stem cells. *Mol Cell Neurosci*. 2013;56:355-64.

246. Yang YM, Gupta SK, Kim KJ, Powers BE, Cerqueira A, Wainger BJ, et al. A small molecule screen in stem-cell-derived motor neurons identifies a kinase inhibitor as a candidate therapeutic for ALS. *Cell Stem Cell*. 2013;12(6):713-26.
247. Imamura K, Sahara N, Kanaan NM, Tsukita K, Kondo T, Kutoku Y, et al. Calcium dysregulation contributes to neurodegeneration in FTLD patient iPSC-derived neurons. *Scientific Reports*. 2016;6(1):34904.
248. Guillaumet-Adkins A, Yanez Y, Peris-Diaz MD, Calabria I, Palanca-Ballester C, Sandoval J. Epigenetics and Oxidative Stress in Aging. *Oxid Med Cell Longev*. 2017;2017:9175806.
249. Vera E, Bosco N, Studer L. Generating Late-Onset Human iPSC-Based Disease Models by Inducing Neuronal Age-Related Phenotypes through Telomerase Manipulation. *Cell Rep*. 2016;17(4):1184-92.
250. Miller JD, Ganat YM, Kishinevsky S, Bowman RL, Liu B, Tu EY, et al. Human iPSC-based modeling of late-onset disease via progerin-induced aging. *Cell Stem Cell*. 2013;13(6):691-705.
251. Kilpinen H, Goncalves A, Leha A, Afzal V, Alasoo K, Asiford S, et al. Common genetic variation drives molecular heterogeneity in human iPSCs. *Nature*. 2017;546(7658):370-5.
252. Preza E, Hardy J, Warner T, Wray S. Review: Induced pluripotent stem cell models of frontotemporal dementia. *Neuropathology and applied neurobiology*. 2016;42(6):497-520.
253. Finch N, Carrasquillo MM, Baker M, Rutherford NJ, Coppola G, Dejesus-Hernandez M, et al. TMEM106B regulates progranulin levels and the penetrance of FTLD in GRN mutation carriers. *Neurology*. 2011;76(5):467-74.
254. van Blitterswijk M, Mullen B, Nicholson AM, Bieniek KF, Heckman MG, Baker MC, et al. TMEM106B protects C9ORF72 expansion carriers against frontotemporal dementia. *Acta Neuropathol*. 2014;127(3):397-406.
255. Gallagher MD, Suh E, Grossman M, Elman L, McCluskey L, Van Swieten JC, et al. TMEM106B is a genetic modifier of frontotemporal lobar degeneration with C9orf72 hexanucleotide repeat expansions. *Acta Neuropathol*. 2014;127(3):407-18.
256. Klein ZA, Takahashi H, Nishida M, Stagi M, Zhou M, Lam TT, et al. Loss of TMEM106B Ameliorates Lysosomal and Frontotemporal Dementia-Related Phenotypes in Progranulin-Deficient Mice. *Neuron*. 2017;95(2):281-96 e6.
257. Park J, Wetzel I, Mariani I, Dreau D, D'Avanzo C, Kim DY, et al. A 3D human triculture system modeling neurodegeneration and neuroinflammation in Alzheimer's disease. *Nat Neurosci*. 2018;21(7):941-51.
258. Grenier K, Kao J, Diamandis P. Three-dimensional modeling of human neurodegeneration: brain organoids coming of age. *Mol Psychiatry*. 2020;25(2):254-74.
259. Lee HK, Velazquez Sanchez C, Chen M, Morin PJ, Wells JM, Hanlon EB, et al. Three Dimensional Human Neuro-Spheroid Model of Alzheimer's Disease Based on Differentiated Induced Pluripotent Stem Cells. *PLoS One*. 2016;11(9):e0163072.
260. Raja WK, Mungenast AE, Lin YT, Ko T, Abdurrob F, Seo J, et al. Self-Organizing 3D Human Neural Tissue Derived from Induced Pluripotent Stem Cells Recapitulate Alzheimer's Disease Phenotypes. *PLoS One*. 2016;11(9):e0161969.
261. Fong H, Wang C, Knoferle J, Walker D, Balestra ME, Tong LM, et al. Genetic correction of tauopathy phenotypes in neurons derived from human induced pluripotent stem cells. *Stem Cell Reports*. 2013;1(3):226-34.

Highlights

- iPSC-derived neurons with *MAPT* mutations display a range of FTD phenotypes including increased tau phosphorylation, tau mislocalisation, decreased neurite length and increased ROS, however they do not display tau tangles.
- iPSC-derived neurons with *GRN* mutations recapitulate phenotypes seen in *GRN* FTD patients, such as progranulin haploinsufficiency and lysosomal dysfunction. However, TDP-43 mislocalisation and aggregation is not always evident.
- iPSC-derived neurons carrying the hexanucleotide repeat expansion (HRE) in *C9ORF72* recapitulate HRE-related pathology and exhibit disease phenotypes including nucleocytoplasmic transport defects, vulnerability to glutamate excitotoxicity, compromised autophagy, and impaired excitability. Importantly, non-cell-autonomous toxicity mechanisms mediated by patient-derived astrocytes or oligodendrocytes have important roles in disease pathogenesis.
- iPSC-derived neurons have the advantage of endogenous expression of the mutant gene of interest, in the cell type specifically affected by disease. They have been beneficial in studying the molecular mechanisms underpinning FTD in a range of familial mutations.
- iPSC-derived models are 'fetal' in nature and do not recapitulate all key aspects of FTD. In addition inter and intra patient variability, and the cost of iPSC culture limit their usefulness.

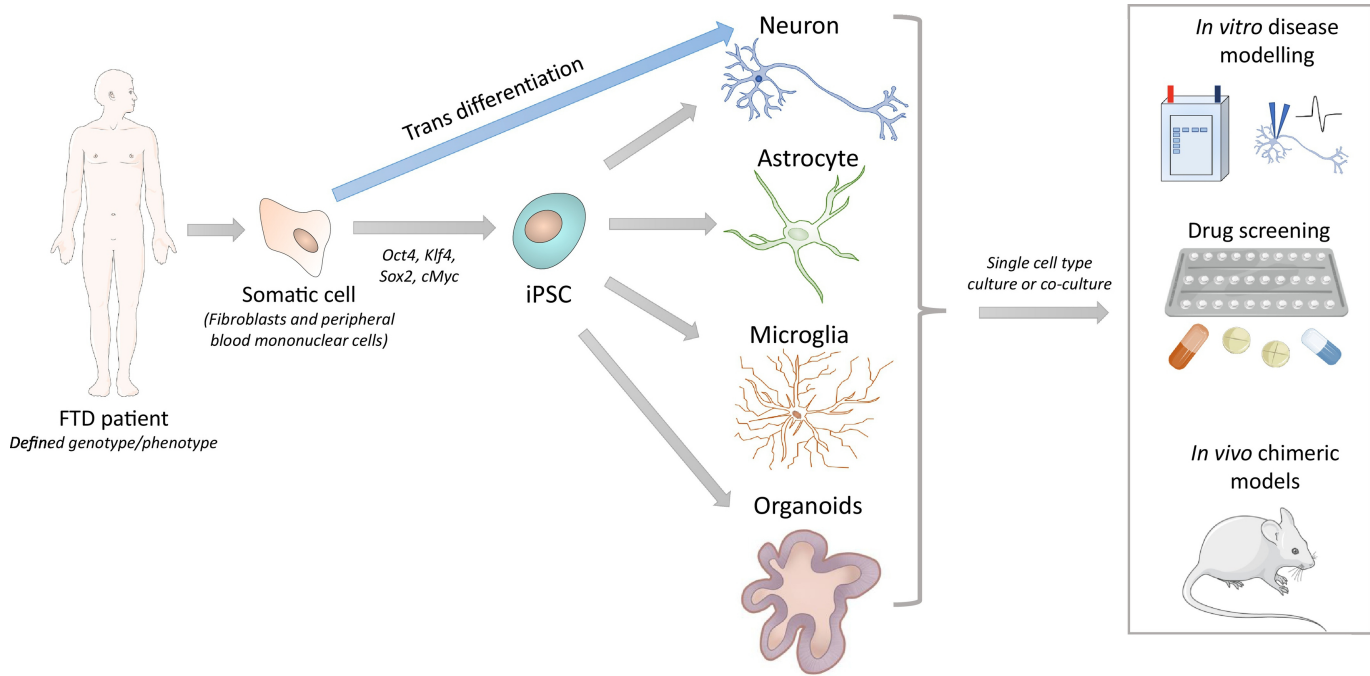


Figure 1

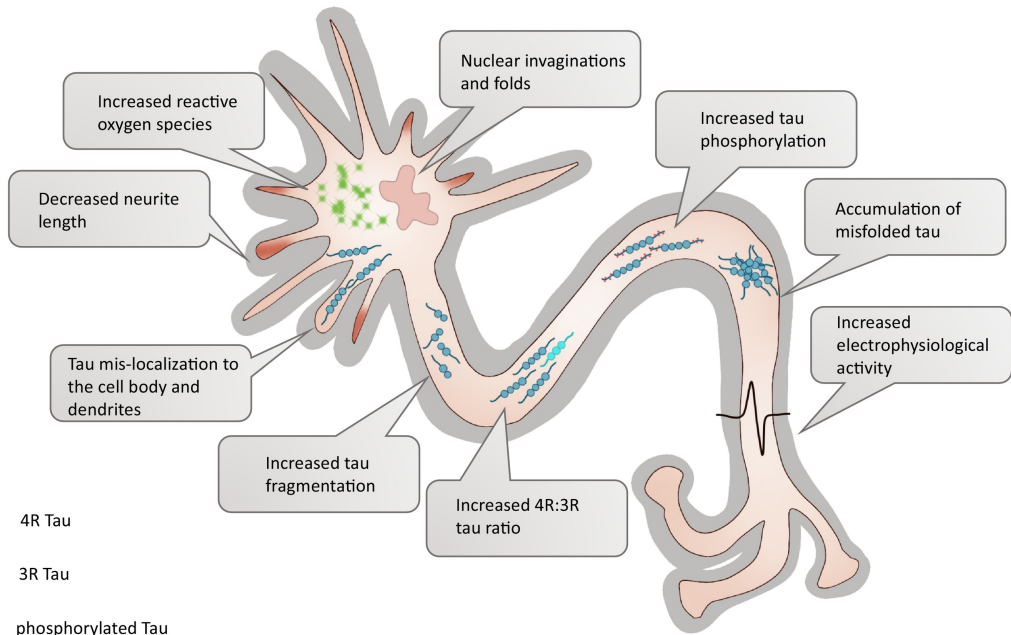


Figure 2

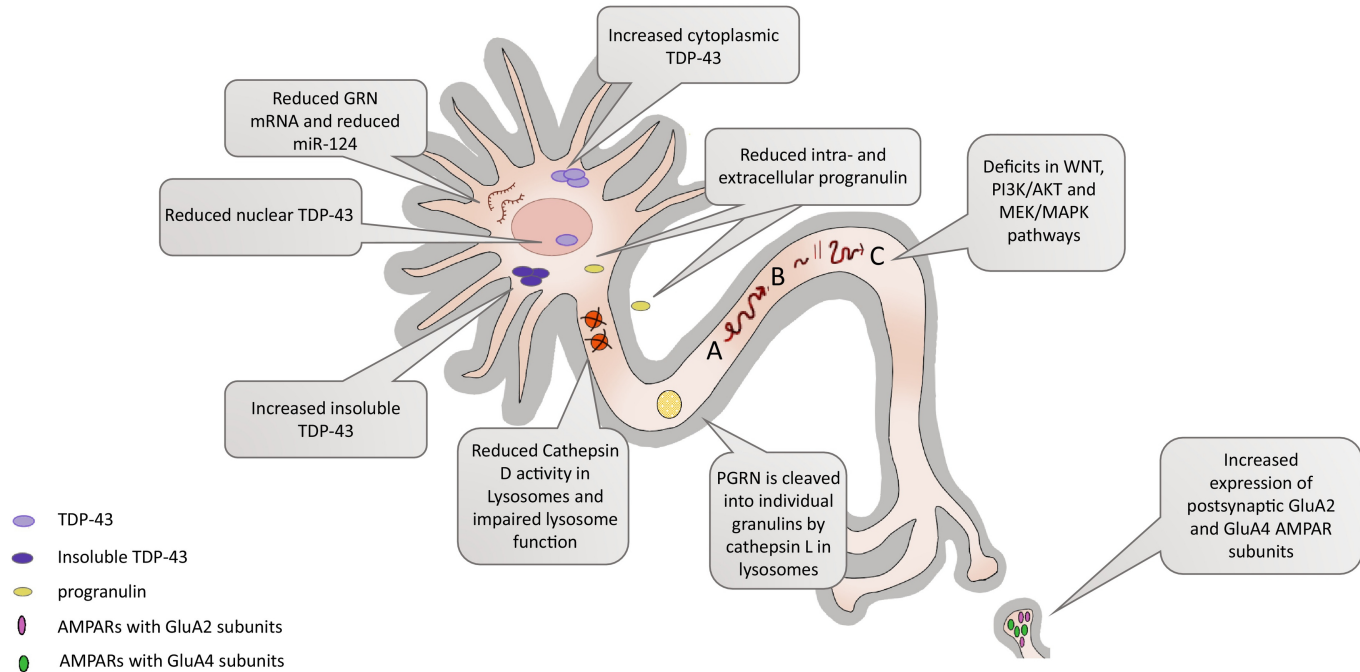


Figure 3

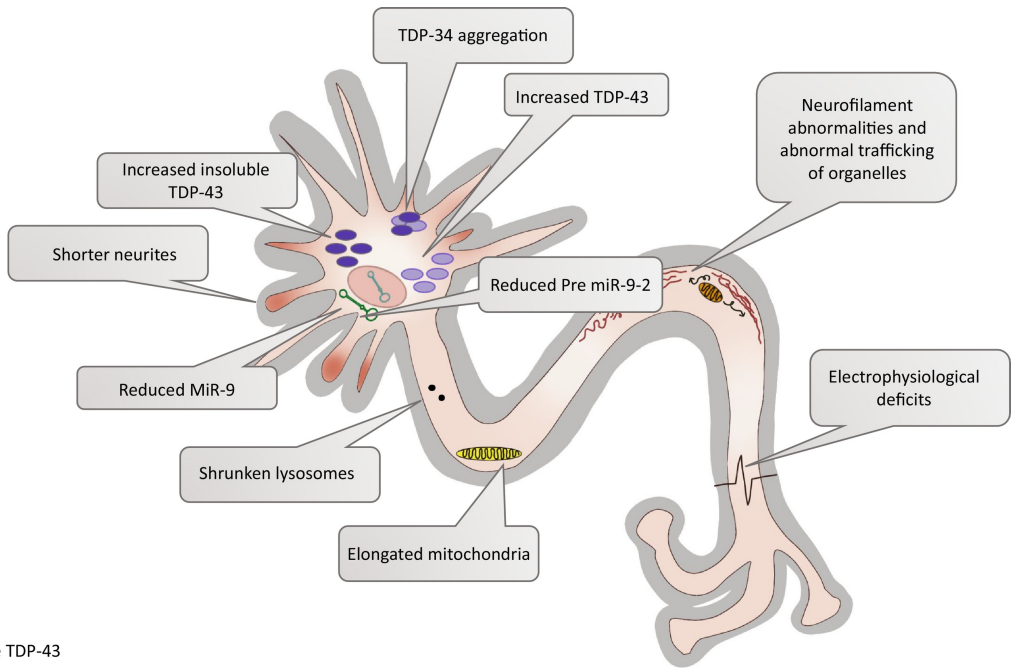


Figure 5